Supporting Information

Cytosolic NQO1 Enzyme-Activated Near-Infrared Fluorescence Imaging and Photodynamic Therapy with Polymeric Vesicles

Chenzhi Yao,[†] Yamin Li,[†] Chengzhou Song,[†] Zhixiong Wang,[‡] Xianglong Hu,*[,‡] and Shiyong Liu*[,†]

[†] CAS Key Laboratory of Soft Matter Chemistry, Hefei National Laboratory for Physical Sciences at the Microscale, Department of Polymer Science and Engineering, University of Science and Technology of China, Hefei, Anhui 230026, China.

[‡] MOE Key Laboratory of Laser Life Science, Institute of Laser Life Science, College of Biophotonics, South China Normal University, Guangzhou 510631, China

***** To whom correspondence should be addressed. E-mail: sliu@ustc.edu.cn, xlhu@scnu.edu.cn

Experimental Section

Materials. Poly(ethylene oxide) monomethyl ether (PEO_{45}-OH, M_n = 2.0 kDa, M_w/M_n = 1.06, mean degree of polymerization, DP, is 45), 7-amino-4-methylcoumarin (AMC), camptothecin (CPT), 2,3,5-trimethylbenzene-1,4-diol, 3-methylbut-2-enoic acid, 3-(4,5-dimethylthiazol-2-yl)-2,5-diphenyltetrazolium bromide (MTT), recombinant human DT diaphorase (NQO1), bovine serum albumin (BSA), and anhydrous potassium carbonate (K_2CO_3) were purchased from Aldrich and used as received. α-Azide-ω-hydroxyl-poly (ethylene oxide) (N_3-PEO_{45}-OH, M_n = 2.0 kDa) was purchased from Suzhou Nord Derivatives Pharm-Tech Co., Ltd. and used as received. Pyridine (99.5%, extra dry over molecular sieves), propylphosphonic anhydride (~50 wt% solution in ethyl acetate), and HCl (4.0 M in MeOH) were purchased from Energy Chemical Co., Ltd. 2-Isocyanatoethyl acrylate (ICEA) (stabilized with BHT), and *tert*-butyldimethylsilyl chloride (TBDMSCl) were purchased from TCI. ICEA was purified by distillation under reduced pressure over phenylmagnesium bromide using CuBr as polymerization inhibitor, and then stored at -20 °C in the glovebox prior to use. Doxorubicin hydrochloride (DOX·HCl) was purchased from Iffect Chemphar Co., Ltd. and used as received. 2-Mercaptoethanol was purchased from Xiya Reagent Co., Ltd. Dicoumarin was purchased from Shanghai Yuanye Technology Co., Ltd. 4-Aminobenzyl alcohol was purchased from Beijing Zhongsheng Huateng Technology Co., Ltd. Fluorescamine (FA), fluorescein diacetate (FDA) and phenylmagnesium bromide (1.0 M solution in THF) were purchased from J&K Scientific Ltd. and used as received. 2-(4-Amidinophenyl)-6-indolecarbamidine dihydrochloride (DAPI), annexin V-FITC apoptosis detection kit, and dihydroethidium (DHE) were purchased from Beyotime Biotechnology Co., Ltd. Fetal bovine serum (FBS), penicillin, streptomycin, and Dulbecco's modified Eagle's medium (DMEM) were purchased from GIBCO and used as received. Triethylamine (TEA) was dried over CaH_2 and distilled prior to use. Dibenzocyclooctyne-maleimide (DBCO-*Mal*) was purchased from Click Chemistry Tools Co., Ltd. The tumor cell-targeting peptide, cyclo(Arg-Gly-Asp-D-Phe-Cys) (*c*RGD), was purchased from Sangon Biotechnology Co., Ltd. Dibenzocyclooctyne-Cy5 (DBCO-Cy5) was purchased from Lumiprobe Co., Ltd. 4,4'-Azobis(4-cyanovaleric acid) (V501) and 2,2′-azoisobutyronitrile (AIBN) were purified by

recrystallization from 95% ethanol prior to use. Nicotinamide adenine dinucleotide (NADH) and 2',7'-dichlorodihydrofluorescein diacetate (DCFH-DA) were purchased from Aladdin. Copper(I) bromide (CuBr), dibutyltin dilaurate (DBTL), anhydrous magnesium sulfate ($MgSO_4$), methanesulfonic acid, *N*-bromosuccinimide (NBS), imidazole, isobutyl chloroformate, dicyclohexyl carbodiimide (DCC), 4-dimethylaminopyridine (DMAP), *N*-methyl morphorline, sodium borohydride ($NaBH_4$), 1,4-dioxane, ethyl acetate (EtOAc), acetonitrile (MeCN), dichloromethane (DCM), tetrahydrofuran (THF), methanol, acetone, ethanol, diethyl ether, *N,N*-dimethylformamide (DMF), dimethyl sulfoxide (DMSO), *n*-hexane, and all other reagents were purchased from Sinopharm Chemical Reagent Co. Ltd. and used as received. Tetrahydrofuran (THF) was dried over sodium wire and distilled just prior to use. Water was deionized with a Milli-Q SP reagent water system (Millipore) to a specific resistivity of 18.4 MΩ·cm.

S-Ethyl-*S*-(α,α′-dimethyl-α″-acetic acid)trithiocarbonate (EMP),[1] N-(4-(hydroxyl-methyl)phenyl)-3-methyl-3-(2,4,5-trimethyl-3,6-dioxocyclohexa-1,4-dien-1-yl)butanamide (TMQH),[2] 3-((9-(diethylamino)-5H-benzo[a]phenothiazin-5-ylidene)amino)propan-1-ol (EtNBS-OH, **D1**),[3] 2-azidoethanol,[4] 3-(4-bromo-2,5-dimethyl-3,6-dioxocyclohexa-1,4-dien-1-yl)-3-methylbutanoic acid (**C2**),[5] and alkynyl-functionalized DOTA-*Gd* complex, *alkynyl*-DOTA-*Gd* (DOTA: 1,4,7,10-tetraazacyclododecane-1,4,7,10-tetrakisacetic acid)[6] were synthesized according to previously reported literature procedures.

Methods. Synthetic routes employed for the preparation of small molecule precursors, amphiphilic block copolymers (PEO-*b*-PTMQ), dye-conjugated amphiphilic block copolymers (BCPs) including PEO-*b*-(PTMQ-*co*-CMA) and PEO-*b*-P(TMQ-*co*-EtNBS), Gd complex-conjugated PEO-*b*-P(TMQ-*co*-*Gd*), and Cy5/cRGD-conjugated vesicle nanoassemblies are shown in Schemes S1-S3.

Synthesis of TMQH Precursor (Scheme S1a). TMQH was synthesized according to literature procedures.[2] Briefly, methanesulfonic acid (30 mL) was heated to 70 ºC in an oil bath, 2,3,5-trimethylbenzene-1,4-diol (3.0 g, 19.7 mmol) and 3-methylbut-2-enoic acid (2.55 g, 22.5 mmol) were then added. The mixture was kept stirring at 70 ºC for 15 h. After cooling to room temperature, deionized water was added to the reaction mixture and then extracted with ethyl

acetate. The combined organic phase was washed with deionized water, saturated aqueous $NaHCO_3$ solution, and saturated aqueous NaCl solution, successively. The organic phase was dried over anhydrous $MgSO_4$, filtered, and then evaporated to dryness under reduced pressure. The obtained off-white crude solid was recrystallized from $CHCl_3$/hexane mixture (3/7, v/v), affording TMQL lactone as a white powder (3.2 g, yield: 69.3%). ^{1}H NMR ($CDCl_3$, δ, ppm, Figure S1a): δ 4.71 (s, 1H), 2.61 (s, 2H), 2.42 (s, 3H), 2.28 (s, 3H), 2.25 (s, 3H), 1.51 (s, 6H).

TMQL (3.0 g, 12.8 mmol), acetonitrile (120 mL), acetone (10 mL), deionized water (60 mL), and NBS (2.28 g, 12.8 mmol) were charged into a reaction flask equipped with a magnetic stirring bar. The resultant mixture was stirred for 30 min at room temperature. After removing most of the organic solvent under reduced pressure, the yellow solid was collected by filtration, washed with deionized water and dried overnight at room temperature in a vacuum oven, affording TMQC as a solid (2.8 g, yield: 94%).^{1}H NMR (DMSO, δ, ppm, Figure S1b): δ 2.22 (s, 1H), 2.94 (s, 2H), 2.18 (s, 3H), 2.00 (d, J = 1.4 Hz, 6H), 1.47 (s, 6H).

Next, TMQC (2.0 g, 8.0 mmol) and isobutyl chloroformate (1.31 g, 9.6 mmol) were dissolved in dry THF (20 mL) at first. After cooling to 0 °C, *N*-methylmorpholine (1 mL) was added and the resultant mixture was stirred at this temperature for 30 min. 4-Aminobenzyl alcohol (1.18 g, 9.6 mmol) was then added and stirred overnight at room temperature. After filtration, further purification *via* flash chromatography (PE/EA) afforded TMQH as a light yellow solid (2.2 g, yield: 77%). ^{1}H NMR (DMSO-d_6, δ, ppm, Figure S2a): δ 9.87 (s, 1H), 7.40 (d, J = 8.3 Hz, 2H), 7.18 (d, J = 8.3 Hz, 2H), 5.06 (s, 1H), 4.39 (d, J = 5.7 Hz, 2H), 2.93 (s, 2H), 2.04 (s, 3H), 1.88 (d, J = 1.8 Hz, 6H), 1.38 (s, 6H). ^{13}C NMR (DMSO-d_6, δ, ppm, Figure S2b): δ 190.29, 186.74, 170.18, 154.15, 143.46, 137.39, 137.26, 136.58, 136.00, 126.79, 118.93, 62.55, 48.76, 37.59, 28.12, 18.86, 13.69, 12.56, 11.68. ESI-MS (m/z) calc. for $C_{21}H_{25}NO_4$: 378.1781 $[M+H]^+$; found: 378.16699.

General synthetic routes employed for the preparation of quinone trimethyl lock-bridged coumarin derivatives, **C3-C5**, are showed in Scheme S1b. Typical procedures are described below.

*Synthesis of **C1***. 2-Mercaptoethanol (5.0 g, 64.0 mmol), imidazole (5.3 g, 76.9 mmol), and 20 mL dry DCM were charged into a reaction flask equipped with a magnetic stirring bar under

dry N_2 atmosphere. *Tert*-Butyldimethylchlorosilane (11.6 g, 76.9 mmol) in dry DCM (10 mL) was slowly added. The mixture was stirred at room temperature for 4 h. Subsequently, the reaction was quenched with water and extracted with DCM (50 mL), the combined organic phase was washed with water and brine, dried over anhydrous $MgSO_4$, filtered, and concentrated under reduced pressure. Without further purification, the crude product **C1** was obtained as a colorless oil (10.2 g, yield: 91%). ^{1}H NMR ($CDCl_3$, δ, ppm, Figure S3a): 3.75 (t, J = 6.4 Hz, 2H), 2.65 (dd, J = 8.3, 6.4 Hz, 2H): 1.57 (d, J = 8.4 Hz, 1H), 0.92 (s, 9H), 0.10 (s, 6H). ^{13}C NMR ($CDCl_3$, δ, ppm, Figure S3b): 65.03, 27.27, 25.87, 18.28, -5.29).

*Synthesis of **C3***: To a solution of **C1** (250.0 mg, 1.27 mmol) in methanol (5 mL), **C2** (294 mg, 1.53 mmol) and K_2CO_3 (211 mg, 1.53 mmol) were consecutively added. The resulting mixture was protected from light, kept stirring at room temperature, and monitored by TLC until the reaction was completed after ~2 h. The solvent was removed under reduced pressure and the crude product was purified by silica gel column chromatography using PE: EA = 3:1 as the eluent, affording **C3** as a yellow oil (450 mg, yield: 83%). ^{1}H NMR ($CDCl_3$, δ, ppm, Figure S4a): δ 3.77 (t, J = 6.6 Hz, 2H), 3.12 (t, J = 6.6 Hz, 2H), 3.03 (s, 2H), 2.18 (s, 3H), 2.14 (s, 3H), 1.45 (s, 6H), 0.89 (s, 9H), 0.06 (s, 6H). ^{13}C NMR ($CDCl_3$, δ, ppm, Figure S4b): δ 188.26, 183.41, 177.47, 152.40, 147.57, 140.58, 140.08, 140.09, 63.30, 46.93, 37.95, 35.97, 28.66, 25.88, 18.32, 14.87, 14.68, -5.33. ESI-MS (m/z) calc. for $C_{21}H_{34}O_5SSi$: 427.1974 $[M+H]^+$; found: 427.1956.

*Synthesis of **C4***. **C3** (200 mg, 0.47 mmol), 7-amino-4-methylcoumarin (99 mg, 0.57 mmol) and dry DCM (5.0 mL) were charged into a reaction flask equipped with a magnetic stirring bar. After cooling to 0 °C, propylphosphonic anhydride (600 μL, 0.94 mmol) and anhydrous pyridine (300 μL) were added, the resulting mixture was stirred at 0 °C overnight. After quenching the reaction with water (50 mL), the mixture was extracted with DCM (2 × 50 mL) and the combined organic layers were washed with water and brine consecutively, then dried over anhydrous $MgSO_4$, filtered. After removing all the solvent under reduced pressure, the crude product was purified by flash column chromatography using PE: EA = 2:1 v/v as the eluent, affording **C4** as a yellow solid (210 mg, yield: 77%). ^{1}H NMR ($CDCl_3$, δ, ppm, Figure S5a): δ 7.70 (s, 1H), 7.56-7.43 (m, 3H), 6.16 (d, J = 1.4 Hz, 1H), 3.75 (t, J = 6.5 Hz, 2H), 3.12-3.02 (m, 4H), 2.36 (d, J = 1.3 Hz, 3H), 2.14 (s, 3H), 2.10 (s, 3H), 1.45 (s, 6H), 0.83 (s, 9H),

0.06 (s, 6H). ^{13}C NMR ($CDCl_3$, δ, ppm, Figure S5b): δ 170.65, 154.14, 153.04, 152.41, 147.79, 141.30, 139.43, 125.29, 116.05, 115.57, 113.32, 106.87, 77.21, 63.28, 50.25, 38.50, 36.09, 28.97, 25.89, 18.60, 18.33, 15.01, 14.56, -5.31. ESI-MS (m/z) calc. for $C_{31}H_{41}NO_6SSi$: 584.2502 $[M+H]^+$; found: 584.2470.

*Synthesis of **C5***: **C4** (100 mg, 0.17 mmol) was dissolved in 10 mL DCM at first. After cooling to 0 ºC, HCl (4 M in MeOH, 2 mL) was added dropwise. The mixture was stirred at room temperature for 30 min and then diluted with DCM (50 mL), washed with aqueous saturated $NaHCO_3$ (50 mL), aqueous saturated NaCl (50 mL), and dried over anhydrous Na_2SO_4. The solvent was removed under reduced pressure and the residues were purified by silica gel column chromatography (PE: EA = 1:1 v/v), affording **C5** as a yellow solid (60 mg, yield: 75%). ^{1}H NMR ($CDCl_3$, δ, ppm, Figure S6a): δ 7.94 (s, 1H), 7.64-7.50 (m, 3H), 6.23 (s, 1H), 3.76 (t, *J* = 5.6 Hz, 2H), 3.11 (d, *J* = 7.4 Hz, 4H), 2.42 (s, 3H), 2.20 (d, *J* = 6.5 Hz, 6H), 1.510 (s, 6H). ^{13}C NMR ($CDCl_3$, δ, ppm, Figure S6b): δ 188.95, 183.95, 170.98, 161.30, 154.08, 152.65, 150.57, 141.34, 138.94, 138.74, 125.36, 116.09, 115.69, 113.27, 106.94, 61.76, 50.15, 38.35, 37.14, 28.66, 18.63, 15.31, 14.55. ESI-MS (m/z) calc. for $C_{25}H_{28}NO_6S$: 470.1637 $[M+H]^+$; found: 470.1613. Elemental Analysis: Calc. for $C_{25}H_{27}NO_6S$: C 63.94%, H 5.80%，N 2.98%, S 6.81%; found: C 64.22%, H 5.89%, N 2.91%, S 6.76%.

General synthetic routes employed for the preparation of quinone trimethyl lock-bridged Nile blue derivatives, **D2-D3**, are showed in Scheme S1c. Typical procedures are described below.

*Synthesis of **D2***. **C2** (96 mg, 0.31 mmol), **D1** (120 mg, 0.31 mmol), DMAP (7.4 mg, 0.031 mmol), and anhydrous DCM (5 mL) were charged into a reaction flask. After cooling to 0 ºC, DCC (126 mg, 0.62 mmol) was added into the mixture. The resulting mixture was protected from light and kept stirring at room temperature for 48 h. Finally, the solvent was removed under reduced pressure and the crude product was purified by flash column chromatography using DCM:CH_3OH = 95:5 as the eluent, affording **D2** as a blue solid (120 mg, yield: 57%). ^{1}H NMR (CD_3OD, δ, ppm, Figure S7a): δ 9.15 – 9.10 (m, 1H), 8.32 (d, *J* = 8.2 Hz, 1H), 8.08 (d, *J* = 9.5 Hz, 1H), 7.92 (t, *J* = 7.8 Hz, 1H), 7.83 (td, *J* = 7.7, 7.1, 1.4 Hz, 1H), 7.44 (dd, *J* = 9.6, 2.8 Hz, 1H), 7.35 (s, 1H), 7.30 (d, *J* = 2.8 Hz, 1H), 4.20 (t, *J* = 6.1 Hz, 2H), 3.81-3.66 (m, 7H), 2.89

(s, 2H), 2.12 (s, 3H), 1.97 (s, 3H), 1.38-1.31 (m, 14H).[13]C NMR (CD_3OD, δ, ppm, Figure S7b): δ 187.21, 179.43, 172.90, 153.21, 151.43, 148.40, 140.09, 138.17, 137.23, 133.86, 133.63, 133.06, 132.16, 130.91, 129.41, 124.99, 124.22, 122.08, 117.58, 104.82, 101.71, 61.83, 53.42, 45.53, 40.92, 37.92, 27.48, 15.91, 13.92, 11.71. ESI-MS (m/z) calc. for $C_{36}H_{38}BrN_3O_4S$: 688.1845 $[M+H]^+$; found: 688.1844.

*Synthesis of **D3***: **D2** (60 mg, 0.087 mmol), 2-mercaptoethanol (7.4 mg, 0.096 mmol), and CH_3OH (5 mL) were charged into a reaction flask, followed by the addition of K_2CO_3 (13.2 mg, 0.096 mmol). The resulting mixture was protected from light and kept stirring at room temperature for ~2 h to complete the reaction, as monitored by TLC. All the solvent was removed under reduced pressure and the crude product was purified by flash column chromatography using DCM:CH_3OH = 95:5 as the eluent, affording **D3** as a blue solid (50 mg, yield: 82%). [1]H NMR (CD_3OD, δ, ppm, Figure S8a): δ 9.14 (dd, *J* = 8.1, 1.3 Hz, 1H), 8.33 (d, *J* = 8.2 Hz, 1H), 8.09 (d, *J* = 9.5 Hz, 1H), 7.95 – 7.90 (m, 1H), 7.88 – 7.81 (m, 1H), 7.44 (dd, *J* = 9.5, 2.8 Hz, 1H), 7.36 (s, 1H), 7.31 (d, *J* = 2.8 Hz, 1H), 4.19 (t, *J* = 6.1 Hz, 2H), 3.86 – 3.65 (m, 6H), 3.58 (t, *J* = 6.4 Hz, 2H), 3.19 (q, *J* = 7.3 Hz, 1H), 2.99 (t, *J* = 6.4 Hz, 2H), 2.89 (s, 2H), 2.10 (s, 3H), 1.95 (s, 3H), 1.44 – 1.16 (m, 14H).[13]C NMR (CD_3OD, δ, ppm, Figure S8b): δ 167.89, 152.68, 151.09, 139.55, 136.91, 133.31, 132.98, 132.41, 132.15, 131.61, 131.02, 130.64, 129.66, 129.24, 128.46, 124.77, 123.77, 123.26, 121.91, 119.91, 117.1, 104.62, 101.56, 67.6 , 59.16, 53.46, 45.52, 38.74, 31.35, 28.73, 23.54 , 22.65, 13.06, 11.86, 10.04. ESI-MS (m/z) calc. for $C_{38}H_{44}N_3O_5S_2$: 686.2722 $[M+H]^+$; found: 686.27136. Elemental Analysis: Calc. for $C_{38}H_{43}N_3O_5S_2$: C 66.54%, H 6.32%, N 6.13%, S 9.33%; found: C 66.92%, H 6.39%, N 6.25%, S 9.45%.

Synthesis of PEO-Based macroRAFT Agent: PEO-based macroRAFT agent was synthesized according to slightly modified literature procedures.[1] Small molecule RAFT agent, *S*-ethyl-*S*-(α,α′-dimethyl-α″-acetic acid)trithiocarbonate (EMP) was synthesized at first.[1] [1]H NMR: ($CDCl_3$, δ, ppm, Figure S9a): *δ* 3.30 (q, 2H), 1.73(s, 6H), 1.34 (t, 3H).

Next, PEO_{45}-OH (7.5 g, 3.75 mmol) was charged into a reaction tube equipped with a magnetic stirring bar and placed overnight into a vacuum oven set at 70 ºC; after cooling to room temperature, EMP (1.68 g, 5.63 mmol) and DMAP (91.5 mg, 0.75 mmol) were quickly

charged into the reaction tube and then sealed by a rubber stopper. Anhydrous toluene (20 mL) was charged into the reaction tube, followed by azeotropic distillation under reduced pressure at 30 °C, and this process was repeated twice. Anhydrous DCM (10 mL) was charged into the reaction tube. DCC (1.16 g, 5.63 mmol) and anhydrous DCM (20 mL) were charged into another 100 mL round bottom flask, and this solution was slowly transferred into the above reaction tube *via* a carefully dried double-tipped needle. The reaction tube was subjected to freeze-pump-thaw cycle for three times, sealed under vacuum, and kept stirring at 30 °C for four days. The reaction tube was quenched into liquid nitrogen, filtered, and precipitated into an excess mixture of *n*-hexane and diethyl ether (1/1, v/v). The precipitates were dissolved in DCM again and the dissolution-precipitation cycle was repeated three times. The final product was dried in a vacuum oven at room temperature overnight, yielding a yellow solid (4.5 g, yield: 54%). The molecular weight and molecular weight distribution of PEO-based macroRAFT agent were determined by GPC using THF as the eluent, revealing an M_n of 2.5 kDa and an M_w/M_n of 1.05. The end group functionalization efficiency of PEO-based macroRAFT agent was determined to be ~95% by ^{1}H NMR analysis in $CDCl_3$ (Figure S9b). According to similar procedures, N_3-PEO_{45}-based macroRAFT agent was also synthesized.

Synthesis of Amphiphilic Block Copolymers (Scheme S2). According to previous literature report,[7] quinone moieties could partially inhibit free radical polymerization, thus quinone-containing monomer cannot be directly polymerized *via* controlled free radical polymerization. NQO1-responsive amphiphilic block copolymers were synthesized *via* the combination of RAFT polymerization and post-polymerization modification. Procedures employed for the synthesis of PEO_{45}-*b*-$PTMQ_{20}$ (**PQ2**) are described. Typically, PEO-based macroRAFT agent (73 mg, 0.033 mmol), AIBN (1.1 mg, 0.0066 mmol), and 1 mL toluene were charged into a reaction tube equipped with a magnetic stirring bar, followed by azeotropic distillation under reduced pressure to remove residual water, and this process was repeated for three cycles. ICEA monomer (141 mg, 1.0 mmol) and anhydrous THF (400 μL) were charged into the reaction tube and the mixture was degassed by three freeze-pump-thaw cycles and sealed under vacuum. Upon stirring at 60 °C in an oil bath for 12 h, the reaction tube was opened in the glovebox. The mixture was transferred into another reaction tube containing anhydrous TMQH

(512 mg, 1.5 mmol) and DBTL catalyst (50 μL), sealed by a rubber stopper, and anhydrous THF (10 mL) was then charged into the reaction tube *via* a dry glass syringe. The mixture was kept stirring at 30 ºC for 48 h. Finally, the reaction mixture was concentrated under reduced pressure and precipitated into an excess of diethyl ether. The precipitates were dissolved in THF and the dissolution-precipitation cycle was repeated for three times. The final product was dried in a vacuum oven overnight at room temperature, yielding a light yellow solid product (180 mg, yield: 32%). The molecular weight and molecular weight distribution of PEO-*b*-PTMQ were determined by GPC using THF as the eluent, revealing an M_n of 9.4 kDa and an M_w/M_n of 1.1 (Table 1). The mean DP of PTMQ block was determined to be 20 by ^{1}H NMR in $CDCl_3$ (Figure S10). Thus, the polymer was denoted as PEO_{45}-*b*-$PTMQ_{20}$ (**PQ2**).

Following similar procedures, PEO_{45}-*b*-$PTMQ_{12}$ (**PQ1**), PEO_{45}-*b*-$PTMQ_{32}$ (**PQ3**), photosensitizer-conjugated BCPs (Scheme S2b) including PEO_{45}-*b*-$P(TMQ_{0.95}$-*co*-$CMA_{0.05})_{20}$ (**PQ5**) and PEO_{45}-*b*-$P(TMQ_{0.94}$-*co*-$EtNBS_{0.06})_{16}$ (**PQ6**), and azide-functionalized BCP, N_3-PEO_{45}-*b*-TMQ_{16} (*azide*-**PQ4**) were also synthesized. Considering that the azide moiety of N_3-PEO_{45}-based macroRAFT agent might be unstable upon extended heating at 60 ºC, 2,2′-azobis(4-methoxy-2,4-dimethylvaleronitrile), a room temperature free radical initiator (V70), was used instead of AIBN to initiate RAFT polymerization at 30 ºC for 12 h. Structural parameters of as-synthesized NQO1-responsive amphiphilic block copolymers are summarized in Table 1.

Synthesis of PEO-b-(PTMQ-co-Gd) (Scheme S2c). Typical procedures employed for the synthesis of PEO-*b*-(PTMQ-*co*-*Gd*) are described below. PEO-based macroRAFT agent (73 mg, 0.033 mmol), AIBN (1.1 mg), and toluene (1 mL) were charged into a reaction tube equipped with a magnetic stirring bar. After azeotropic distillation under reduced pressure for three cycles, ICEA monomer (141 mg, 1 mmol) and anhydrous THF (400 μL) were charged into the reaction tube, which was carefully degassed by three freeze-pump-thaw cycles and sealed under vacuum. After stirring at 60 ºC for 12 h, the reaction mixture was opened in the glovebox. The mixture was transferred into another reaction tube containing dry THF (10 mL), anhydrous TMQH (512 mg, 1.5 mmol), 2-azidoethanol (13 mg, 0.15 mmol), and DBTL catalyst (50 μL). The reaction tube was sealed by a rubber stopper under N_2 atmosphere. The reaction

mixture was stirred at 30 ºC for 48 h. Finally, the reaction mixture was concentrated under reduced pressure and then precipitated into an excess of diethyl ether. The above dissolution-precipitation cycle was repeated for three times. The final product was dried in a vacuum oven overnight at room temperature, yielding a light yellow solid product. The total DP of azide-containing block is ~25 based on ^{1}H NMR analysis. The molecular weight and molecular weight distribution of PEO$_{45}$-*b*-P(TMQ-*co*-*N*$_3$)$_{25}$ were determined by GPC using THF as the eluent, revealing an M_n of 12.8 kDa and an M_w/M_n of 1.2 (Table 1).

Next, PEO-*b*-(PTMQ-*co*-*Gd*) was obtained *via* click reaction of alkynyl-functionalized DOTA-*Gd* complex with PEO-*b*-(PTMQ-*co*-*N*$_3$)$_{25}$ precursor polymer. PEO-*b*-(PTMQ-*co*-*N*$_3$)$_{25}$ (0.22 g) and 2 mL THF were charged into a reaction tube, alkynyl-functionalized DOTA-*Gd* complex (2.0 equiv. relative to azide moieties) and sodium ascorbate (2.0 equiv. relative to azide moieties) dissolved in deionized water (100 μL) were then added, followed by the addition of CuBr (2.0 equiv. relative to azide moieties). The reaction mixture was carefully degassed by three freeze-pump-thaw cycles and sealed under vacuum. Upon stirring at room temperature for 48 h, the reaction tube was opened and exposed to air. The mixture was passed through a silica gel column to remove copper catalyst. The resulting mixture was dried over anhydrous $MgSO_4$ and filtered. After removing all the solvents under reduced pressure, the residues were dissolved in DCM and precipitated into an excess of diethyl ether. The above dissolution-precipitation cycle was repeated for three times. The final product was dried in a vacuum oven overnight at room temperature, affording a light yellow solid. 5 mg of the above obtained PEO-*b*-(PTMQ-*co*-*Gd*) diblock copolymer was treated with 1 mL concentrated nitric acid until complete dissolution, the mixture to heated to 110 ºC and evaporated to dryness. After this process was repeated twice, 1 mL deionized water was added and the Gd content was analyzed by inductively coupled plasma-atomic emission spectrometry (ICP-AES). The Gd^{3+} content in the diblock copolymer was determined to be ~2.04 wt%, and the final product was denoted as PEO$_{45}$-*b*-(PTMQ$_{0.92}$-*co*-*Gd*$_{0.08}$)$_{25}$ (Table 1, *Gd*-**PQ7**).

Characterization. All nuclear magnetic resonance (NMR) spectra were recorded on a Bruker AV300 NMR spectrometer operated in the Fourier transform mode using $CDCl_3$, DMSO-d_6, CD_3OD, and D_2O as the solvents. Reversed-phase HPLC (RP-HPLC) analysis was

performed on a Shimadzu HPLC system, equipped with a LC-20AP binary pump, a SPD-20A UV-Vis detector, and a Symmetry C18 column using methanol/H_2O as the mobile phase. Electrospray ionization mass spectrometry (ESI-MS) analysis was performed on a Thermo Fischer Scientific TTQ Orbitrap mass spectrometer equipped with an electrospray interface. Molecular weights (MW) and molecular weight distributions were determined by gel permeation chromatography (GPC) equipped with Waters 1515 pump and Waters 2414 differential refractive index detector (set at 30 ^oC). A series of two linear Styragel columns (HR2 and HR4) were employed with the oven temperature set at 30 ^oC. The eluent was THF at a flow rate of 1.0 mL/min. A series of narrow polydispersity polystyrene standards were employed for calibration. A Zetasizer Nano ZS system (Malvern Instruments Ltd, England) was used for dynamic laser light scattering (DLS) measurements. Scattering light was collected at a fixed angle of 173^o for duration of ~5 min. All data were averaged over three consecutive measurements. UV-Vis absorbance was conducted on a TU-1910 double-beam UV-Vis spectrophotometer (Beijing Puxi General Instrument Co., Ltd.). Fluorescence spectra were recorded on a F4600 (Hitachi) spectrofluorometer. The temperature of water-jacketed cell holder was controlled by a programmable circulation bath. The slit widths were set at 5 nm for both excitation and emission. TEM analysis was conducted on a JEOL 2010 electron microscope. Field-emission scanning electron microscope (FE-SEM) analysis was performed on a high resolution JEOL JSM-6700 field-emission scanning electron microscopy. Fourier transform infrared (FT-IR) spectra were recorded on a Bruker VECTOR-22 IR spectrometer. The spectra were collected over 64 scans with a spectral resolution of 4 cm^{-1}. Inductively coupled plasma atomic emission spectrometry (ICP-AES) (Optima 7300 DV, Perkin Elmer Co., Ltd.) was used for the determination of Gd^{3+} content. Confocal laser scanning microscopy (CLSM) imaging was performed on a Leica TCS SP5 microscopy.

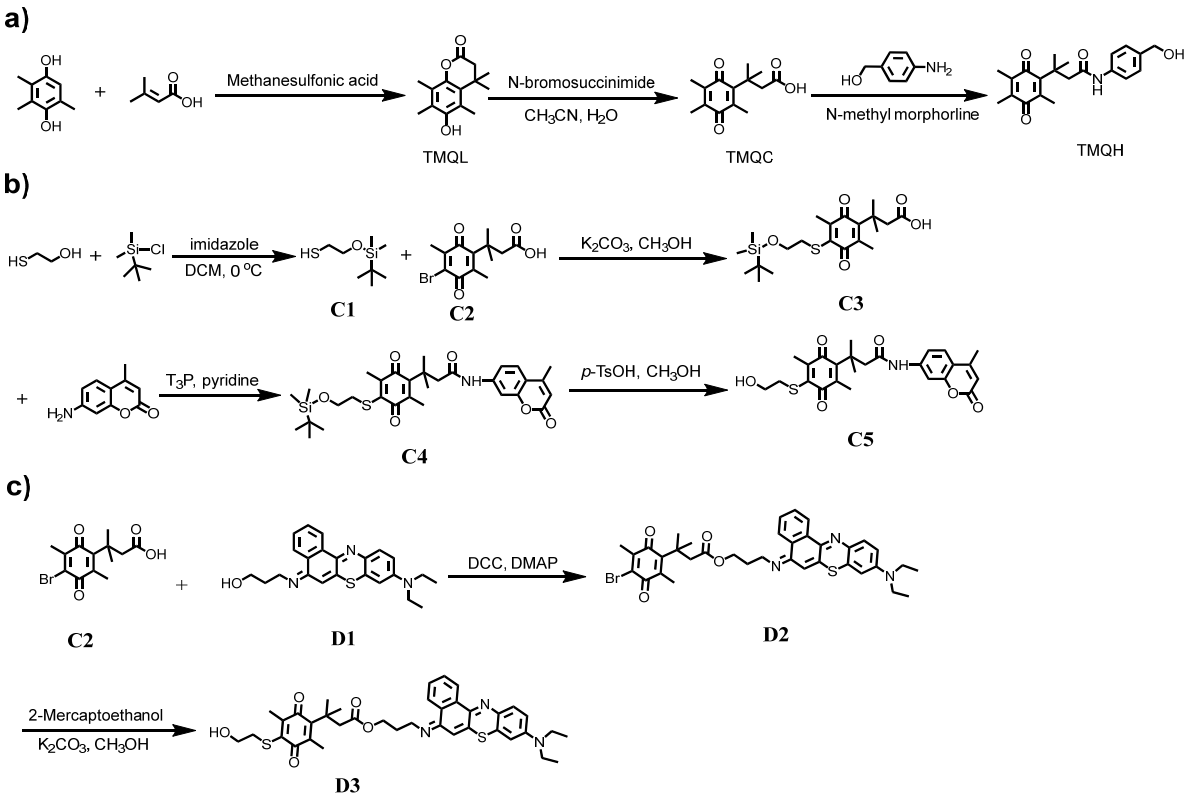

Scheme S1. Synthetic routes employed for the preparation of three types of NQO1-responsive small molecule precursors including **TMQH**, **C5**, and **D3**.

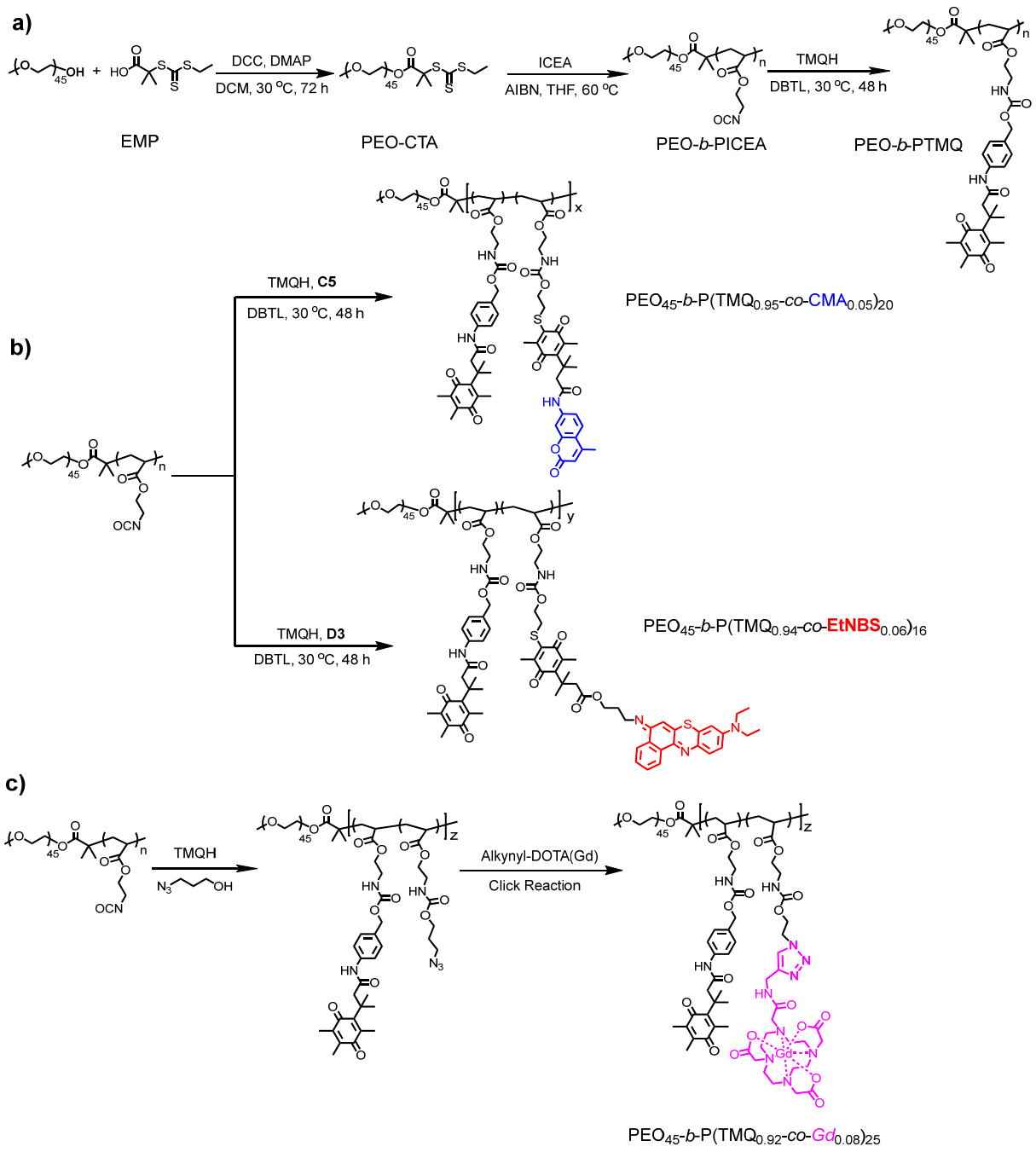

Scheme S2. (a) Synthetic routes employed for the preparation ofPEO-based macroRAFT agent, PEO-CTA, and NQO1-responsive amphiphilic diblock copolymers, PEO-*b*-PTMQ. (b) Synthetic routes employed for the preparation of CMA and EtNBS-conjugated NQO1-responsive diblock copolymers including PEO-*b*-P(TMQ-*co*-CMA) (**PQ5**) and PEO-*b*-(TMQ-*co*-EtNBS) (**PQ6**). (c) Synthetic routes employed for the preparation of DOTA(*Gd*)-functionalized NQO1-responsive diblock copolymers, PEO-*b*-P(TMQ-*co*-*Gd*) (*Gd*-**PQ7**).

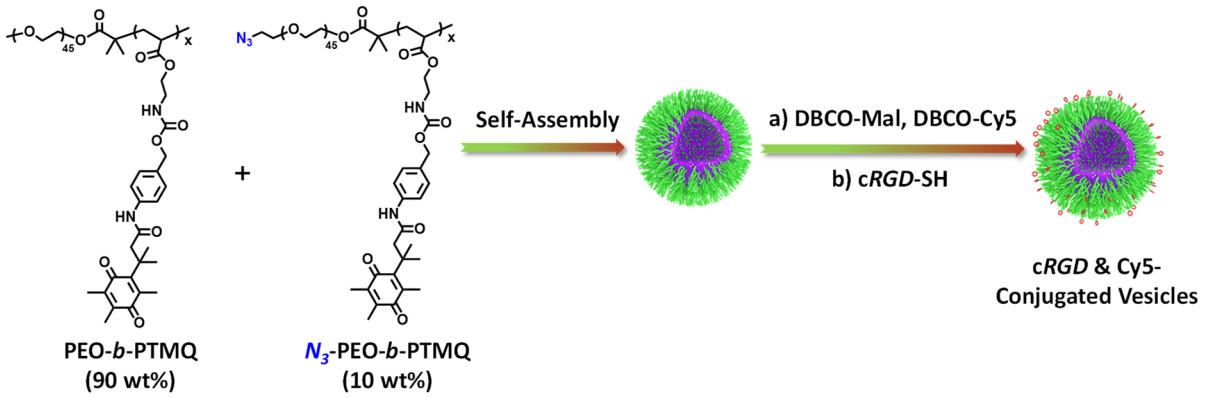

Scheme S3. Schematics of *in situ* fabrication of Cy5 and *c*RGD-conjugated NQO1-responsive vesicular nanoassemblies *via* block copolymer co-assembly and high-efficiency surface conjugation reactions.

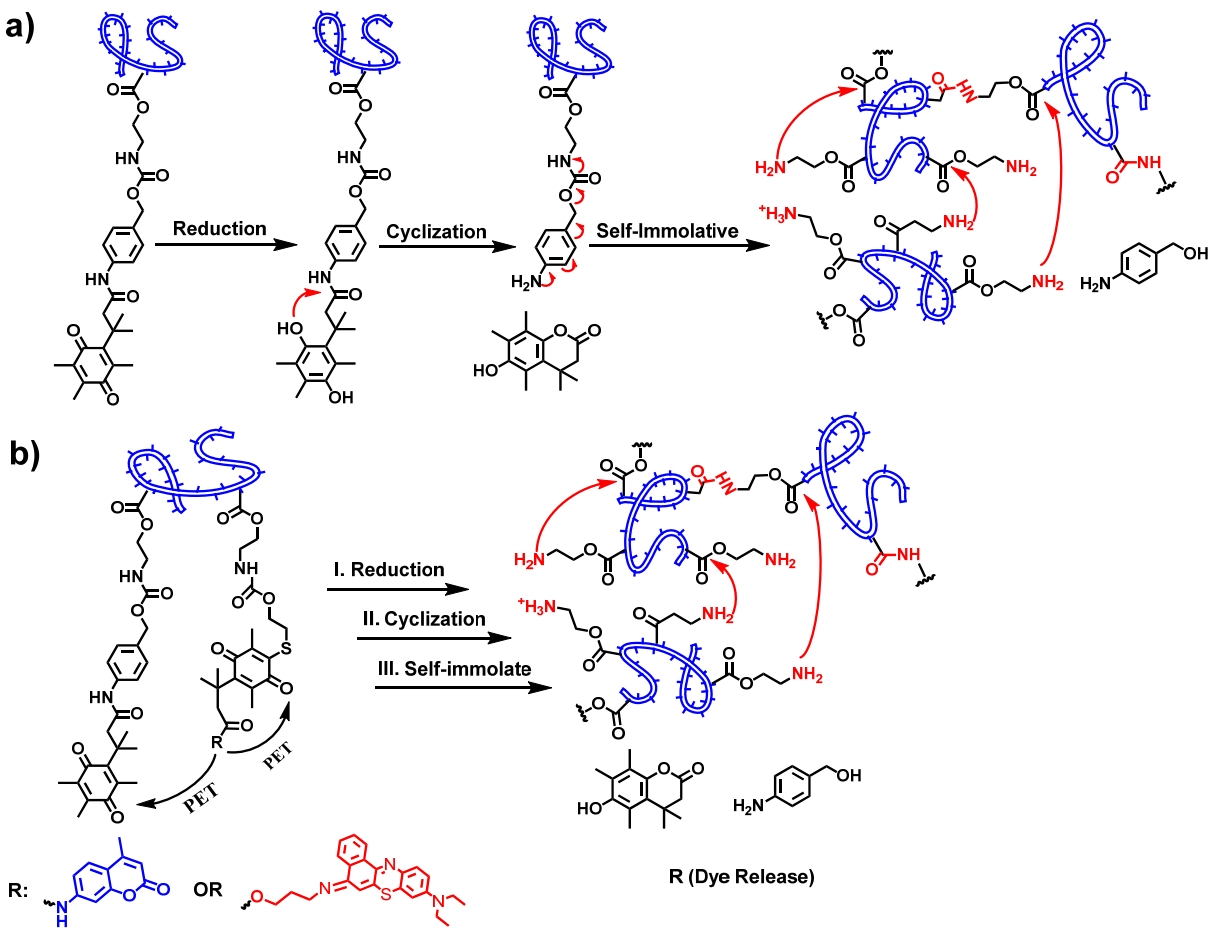

Scheme S4. a) Schematic illustration of enzyme-triggered degradation and intrachain/ interchain crosslinking mechanisms of NQO1-responsive block copolymer vesicular assemblies. b) Upon self-immolative cascade degradation, the PET quenching mechanism was inhibited, accompanied with the turn-on of fluorescence emission due to the release of small molecule coumarin and Nile blue photosensitizers.

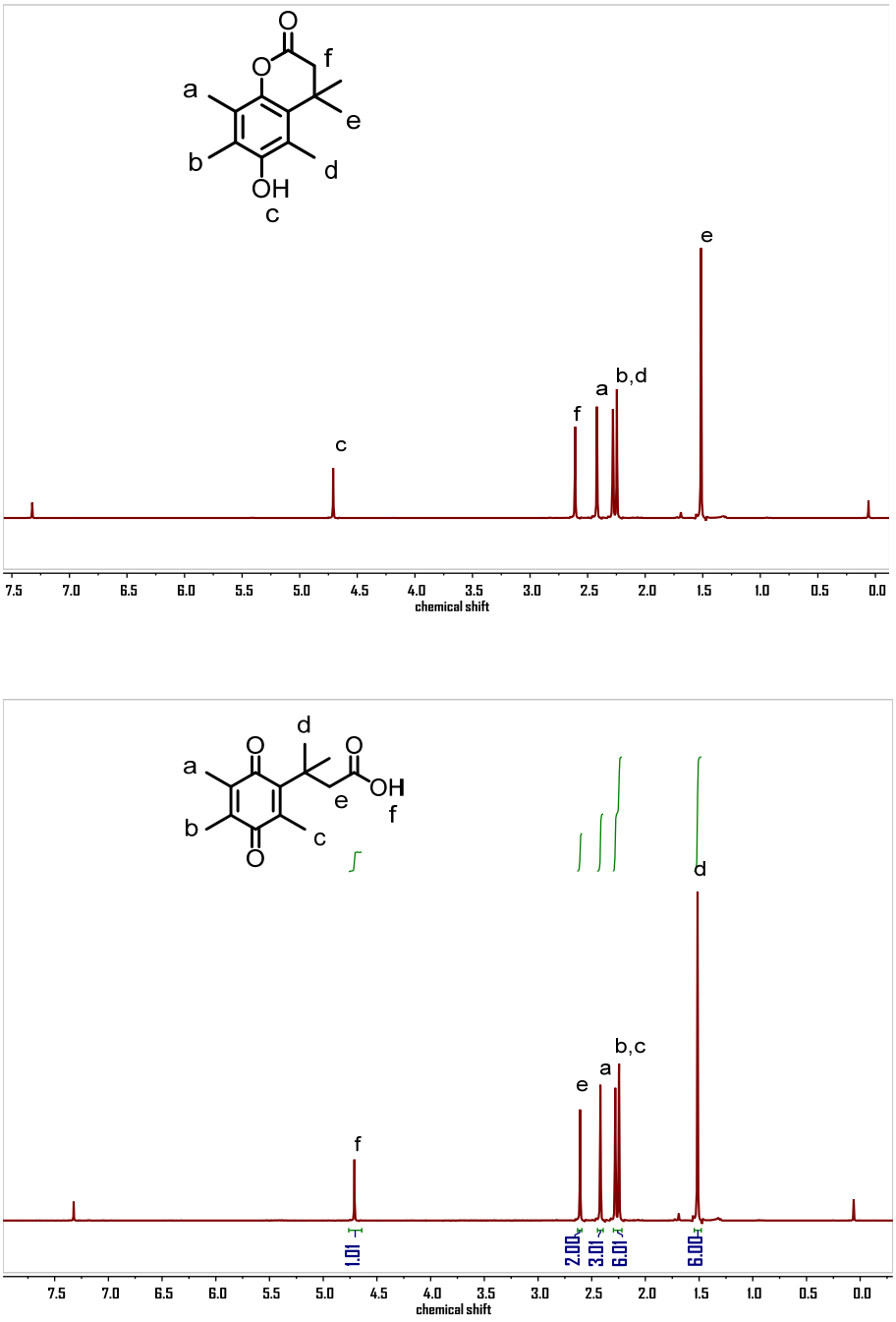

Figure S1. ^{1}H NMR spectra recorded for **TMQL** and **TMQC** in $CDCl_3$, respectively.

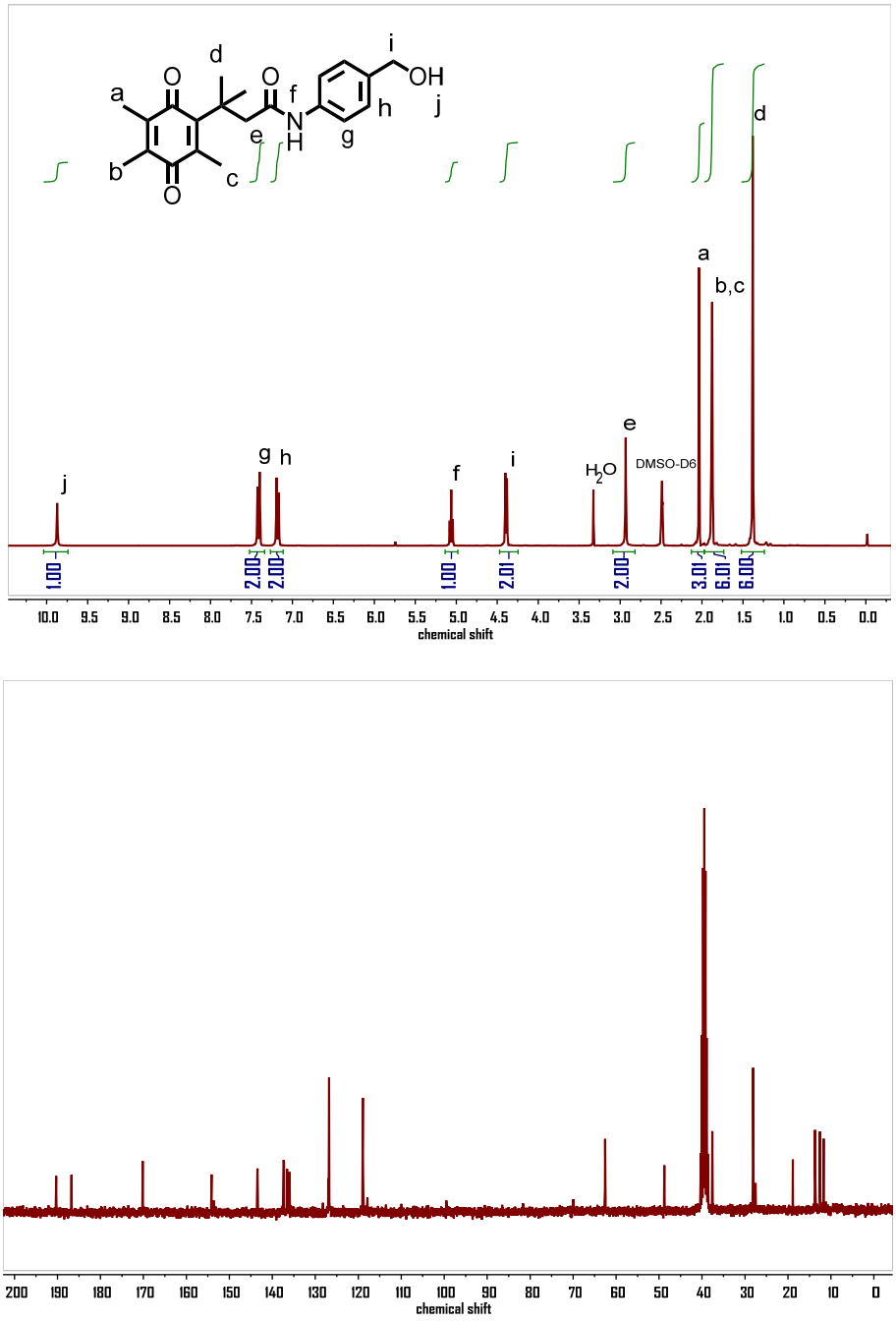

Figure S2. ^{1}H NMR and ^{13}C NMR spectra recorded for **TMQH** in DMSO-d_6.

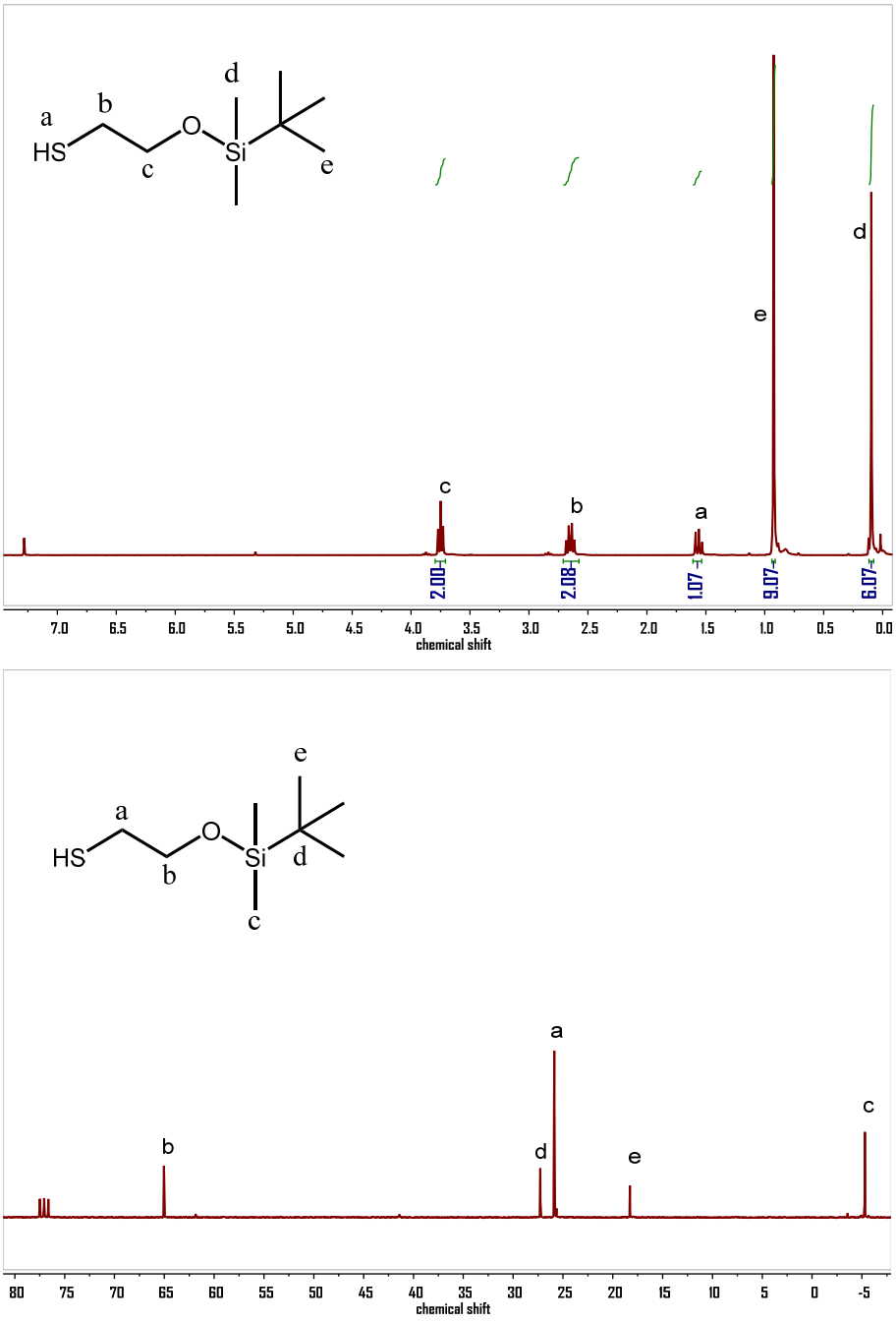

Figure S3. ^{1}H NMR and ^{13}C NMR spectra recorded for **C1** in $CDCl_3$.

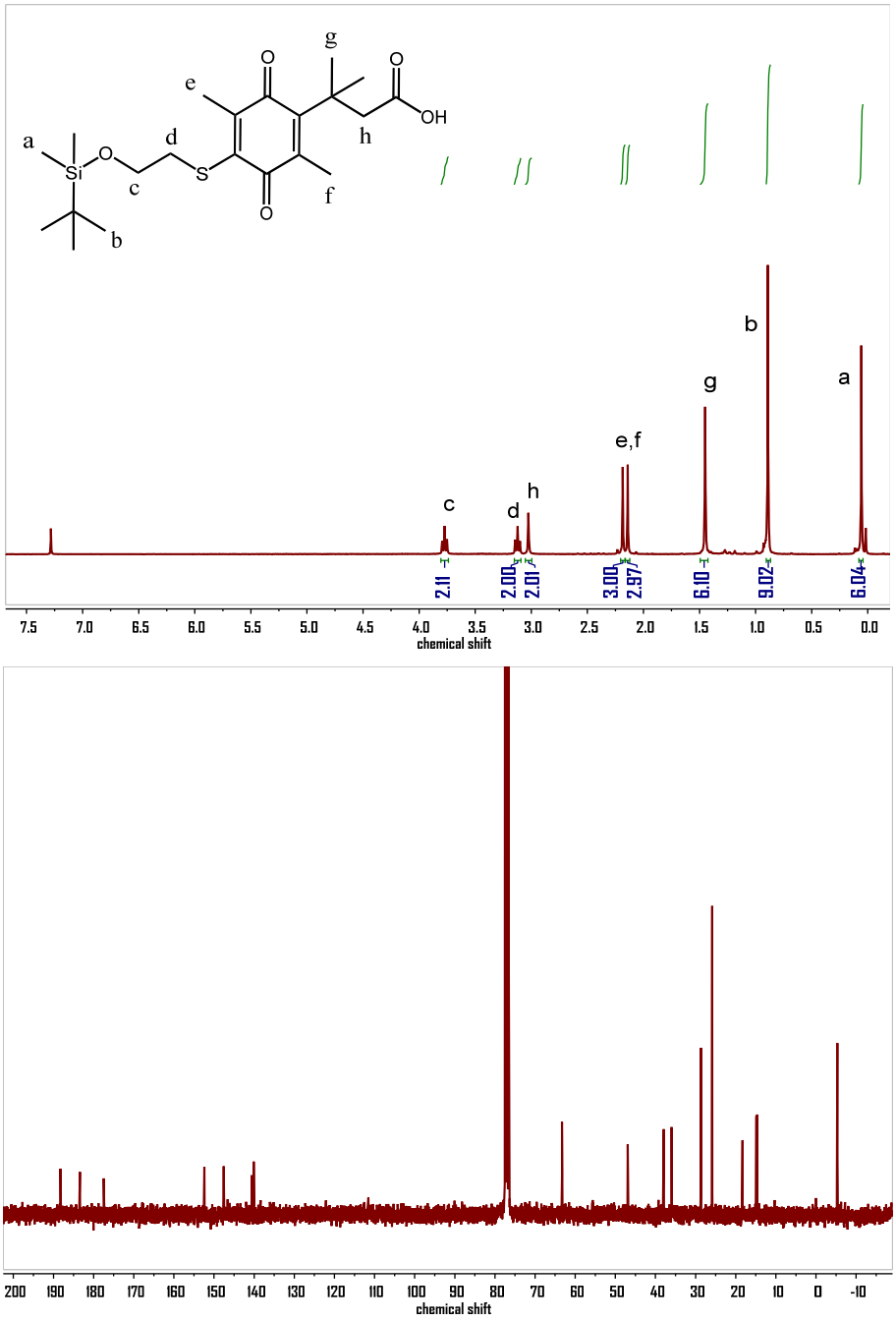

Figure S4. ^{1}H NMR and ^{13}C NMR spectra recorded for **C3** in $CDCl_3$.

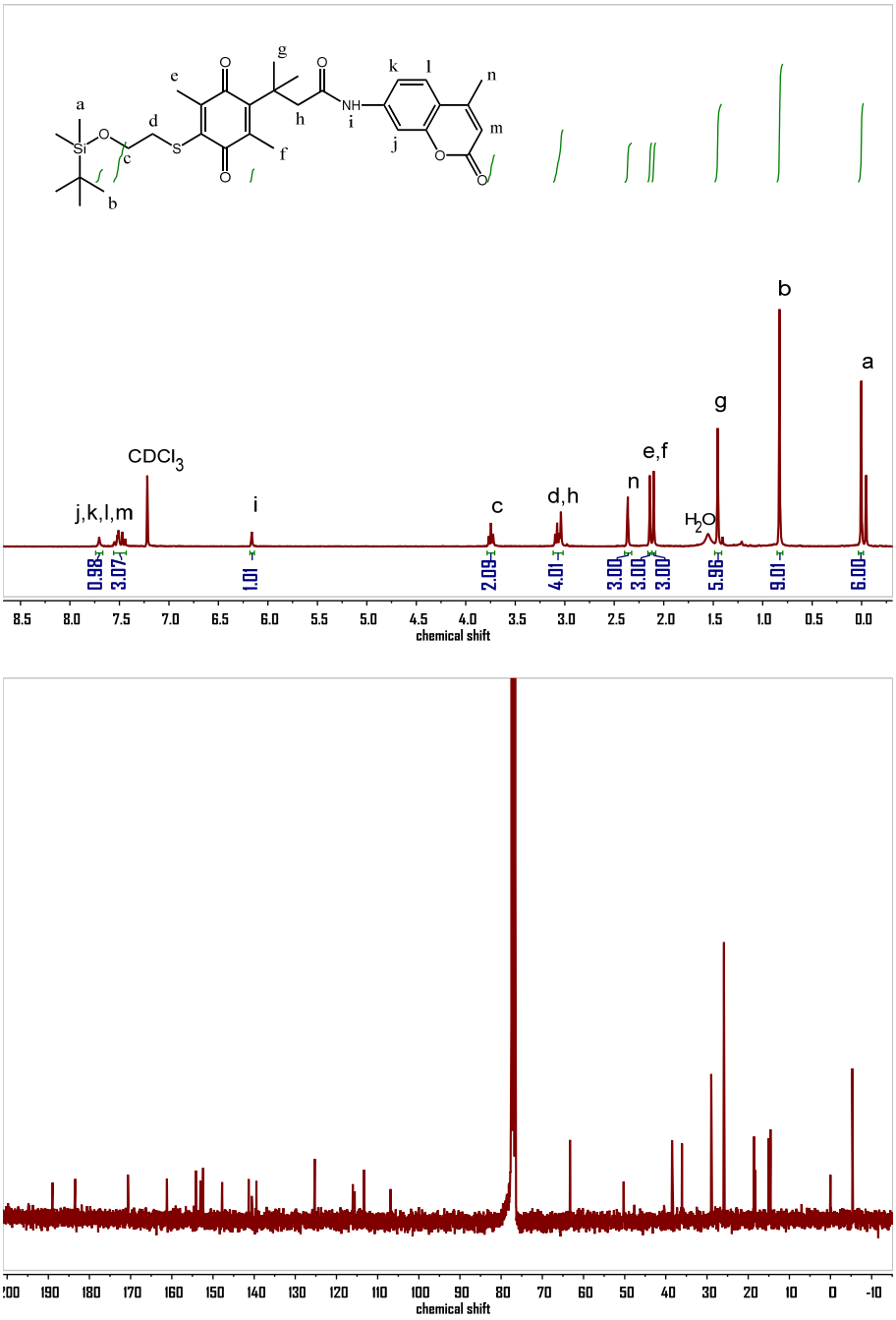

Figure S5. ^{1}H NMR and ^{13}C NMR spectra recorded for **C4** in $CDCl_3$.

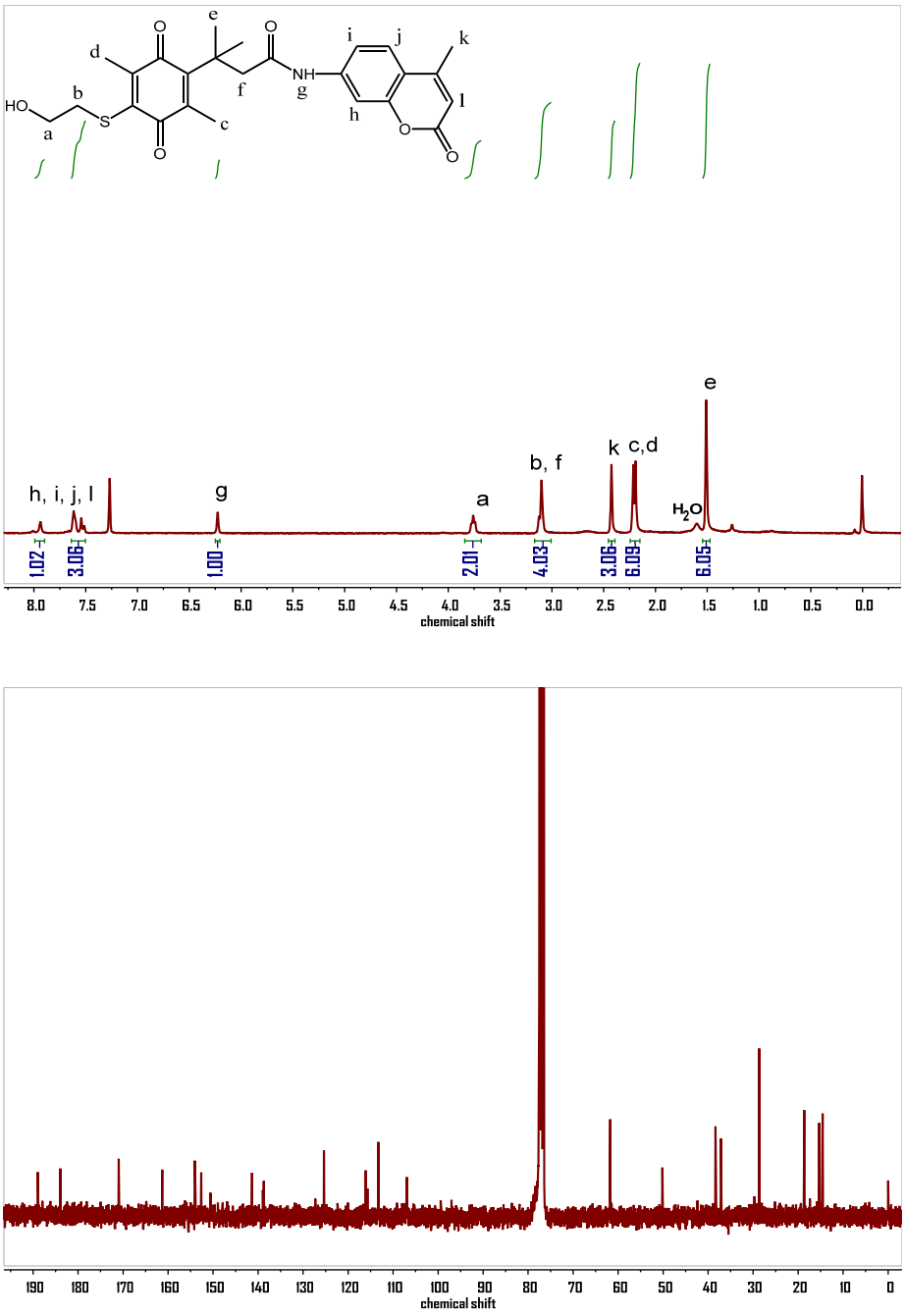

Figure S6. ^{1}H NMR and ^{13}C NMR spectra recorded for **C5** in $CDCl_3$.

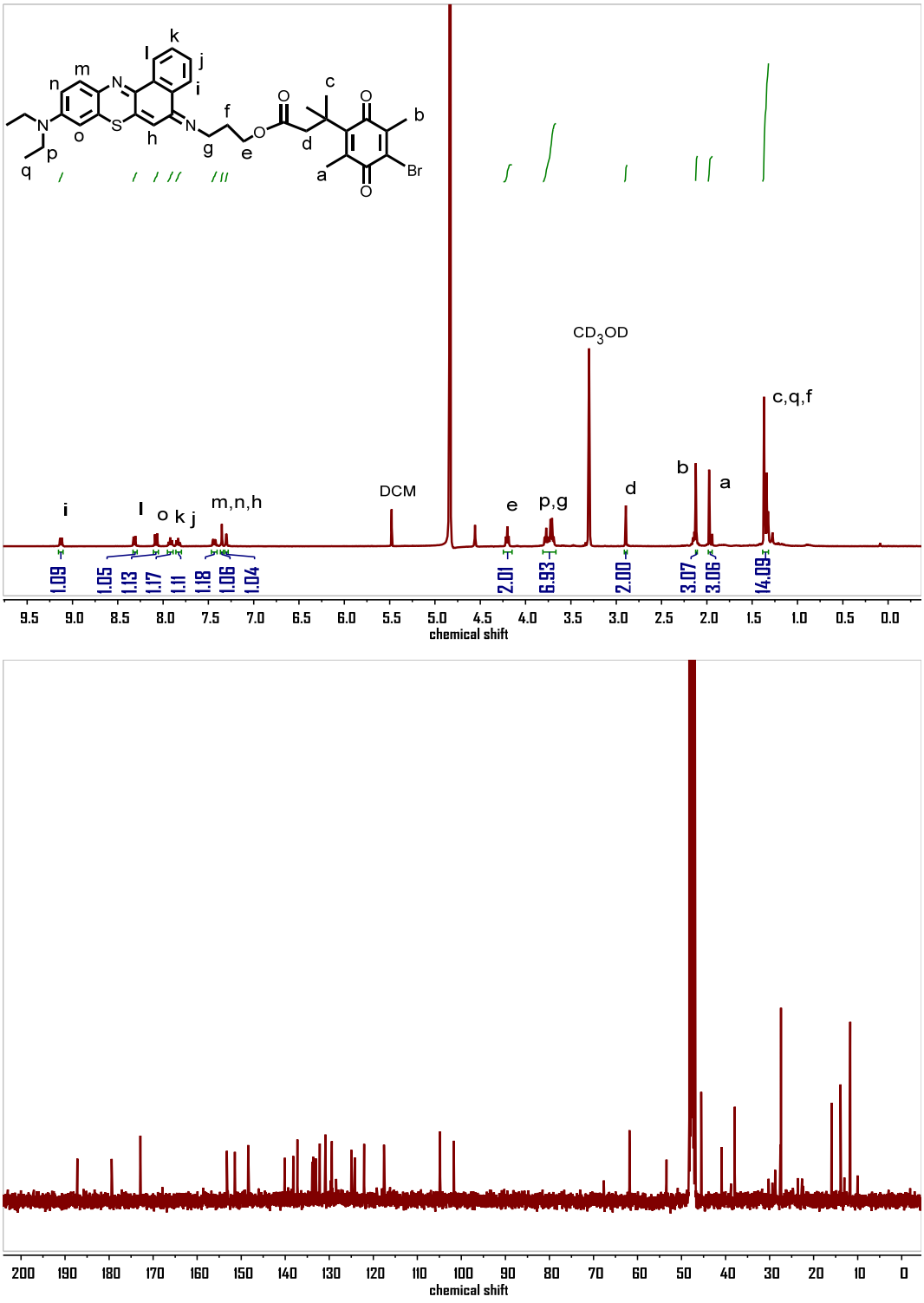

Figure S7. ^{1}H NMR and ^{13}C NMR spectra recorded for **D2** in CD_3OD.

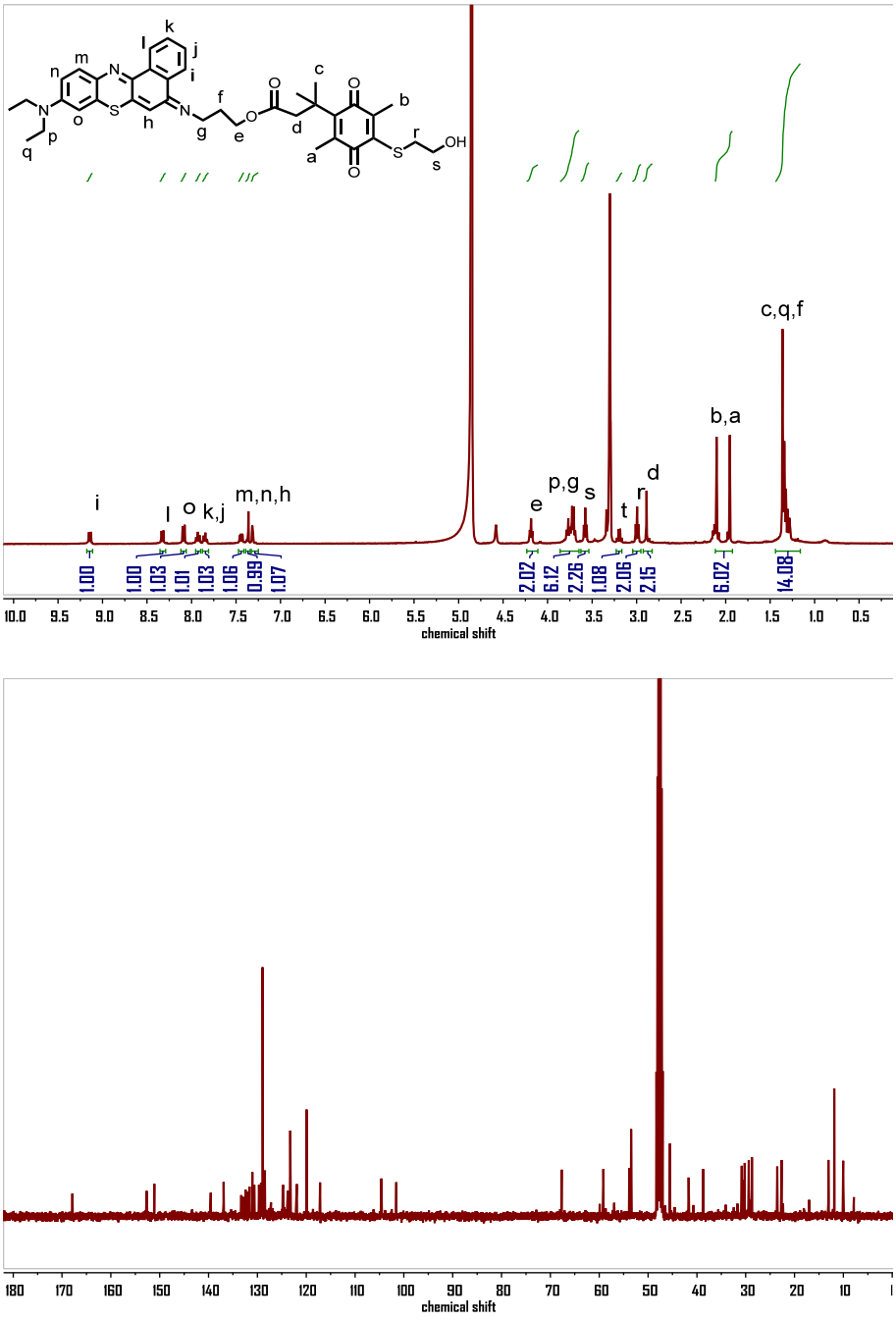

Figure S8. ^{1}H NMR and ^{13}C NMR spectra recorded for **D3** in CD_3OD.

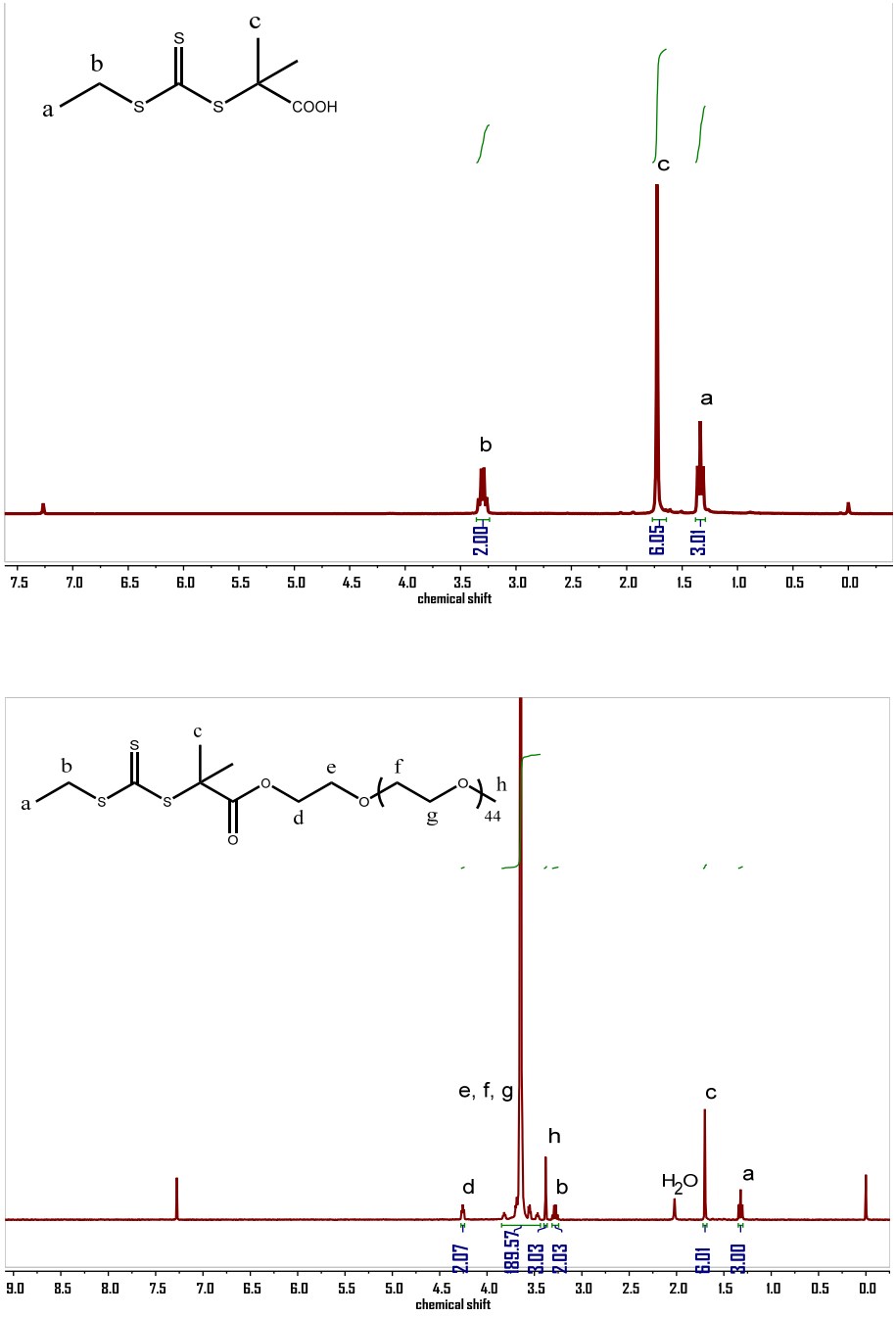

Figure S9. ^{1}H NMR spectra recorded for small molecule RAFT agent, EMP (top), and PEO-based macroRAFT agent (bottom) in $CDCl_3$, respectively.

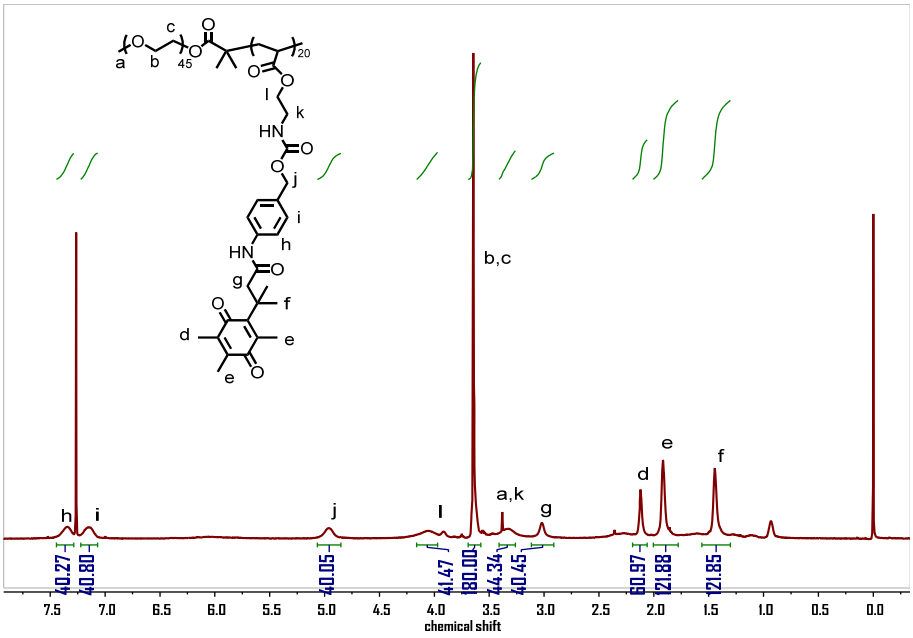

Figure S10. ^{1}H-NMR spectrum recorded for PEO_{45}-*b*-$PTMQ_{20}$ (**PQ2**) in $CDCl_3$.

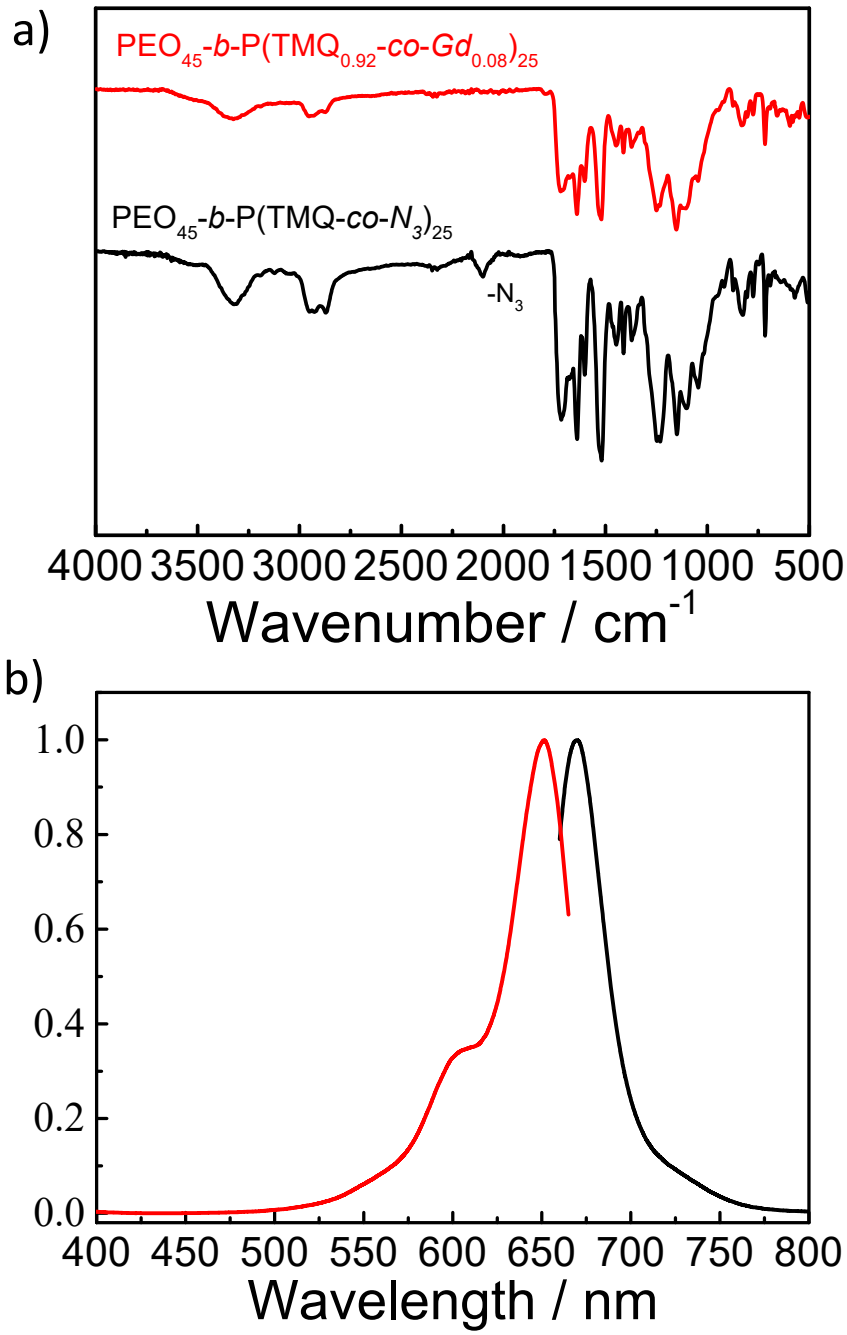

Figure S11. (a) FT-IR spectra recorded for PEO_{45}-*b*-P(TMQ-*co*-N_3)$_{25}$ and PEO_{45}-*b*-P(TMQ$_{0.92}$-*co*-*Gd*$_{0.08}$)$_{25}$, respectively. (b) Fluorescence excitation spectra (red line, λ_{em} = 675 nm) and emission spectra (blank line, λ_{ex} = 650 nm) recorded for the aqueous dispersion of Cy5-conjugated vesicles co-assembled from **PQ2** and *azide*-**PQ4** (9/1, weight ratio).

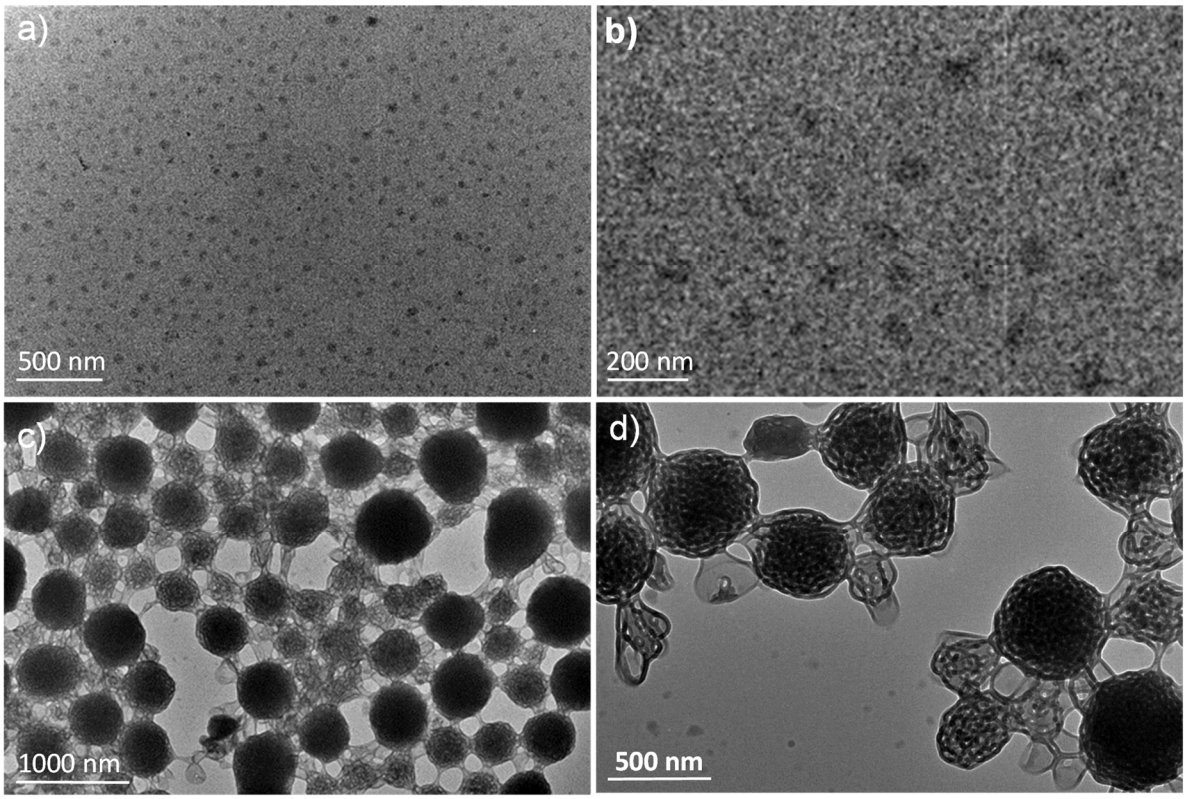

Figure S12. Typical TEM images recorded by drying the aqueous dispersions of (a,b) spherical micelles self-assembled from **PQ1** and (c,d) large compound vesicles (LCVs) self-assembled from **PQ3**.

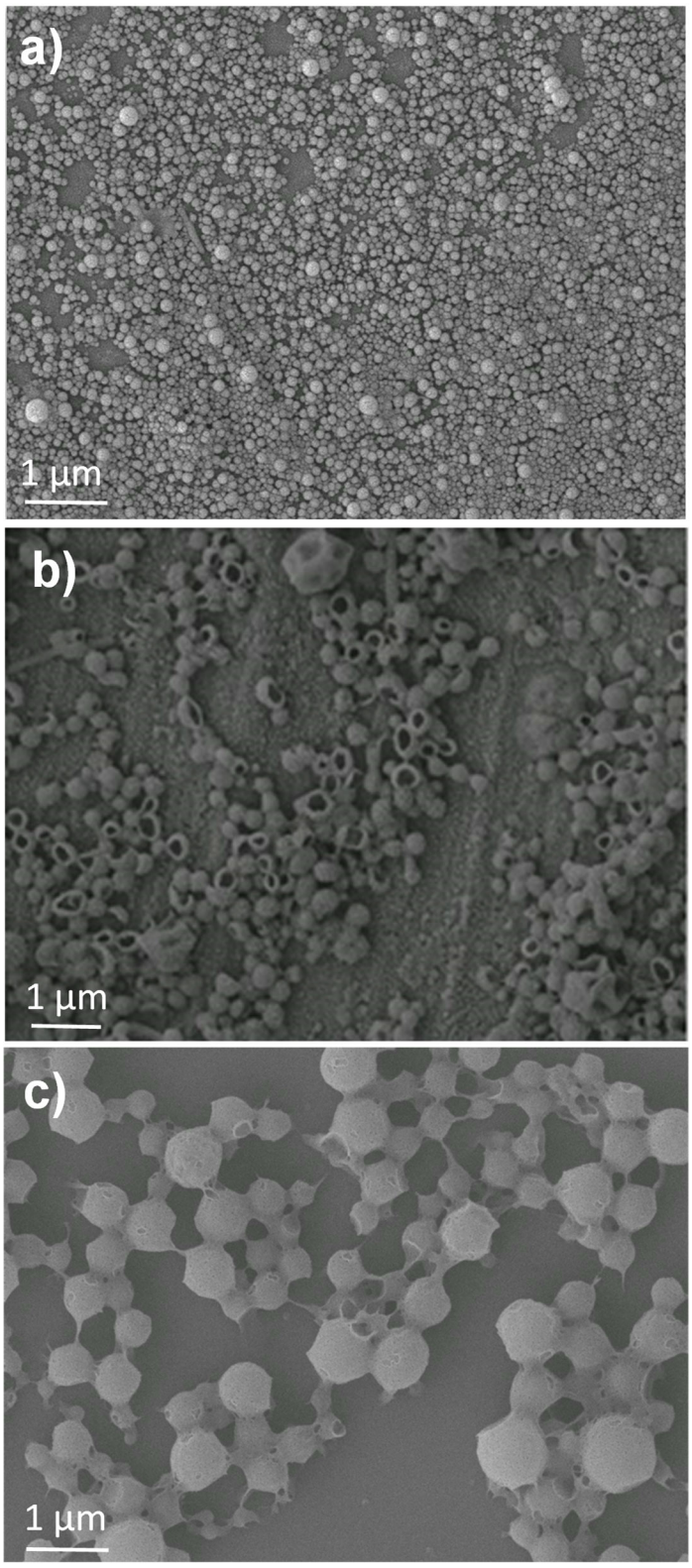

Figure S13. Typical SEM images recorded for (a) spherical micelles of **PQ1**, (b) **PQ2** vesicles, and (c) LCVs of **PQ3**.

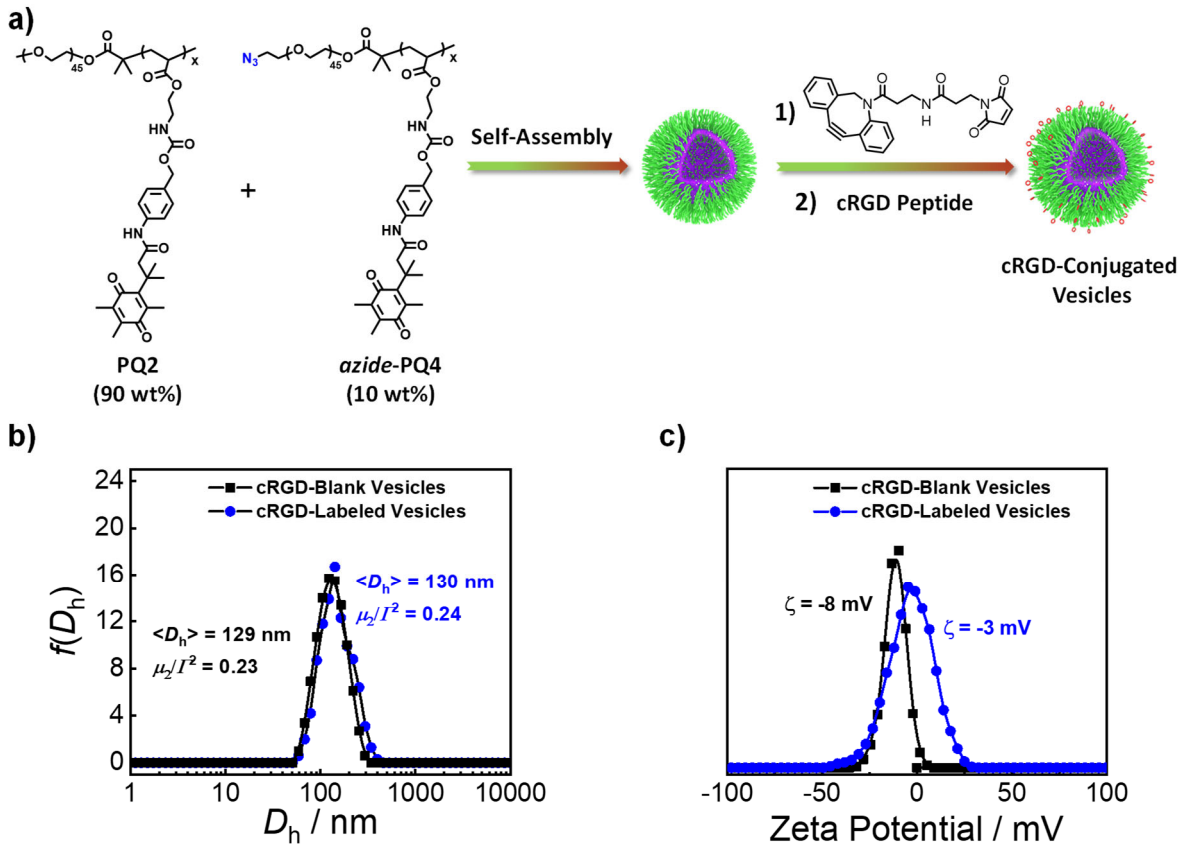

Figure S14. (a) Schematics of the surface modification of azide-functionalized vesicles co-assembled from **PQ2** and *azide*-**PQ4** (9:1 wt/wt) with *c*RGD *via* sequential copper-free "click" and thiol-maleimide Michael addition reactions. (b) Hydrodynamic diameter distributions, $f(D_h)$, and (c) zeta potentials recorded for aqueous dispersions of *c*RGD-blank vesicles of **PQ2** and *c*RGD-functionalized vesicles co-assembled from **PQ2** and *azide*-**PQ4** (9:1 wt/wt).

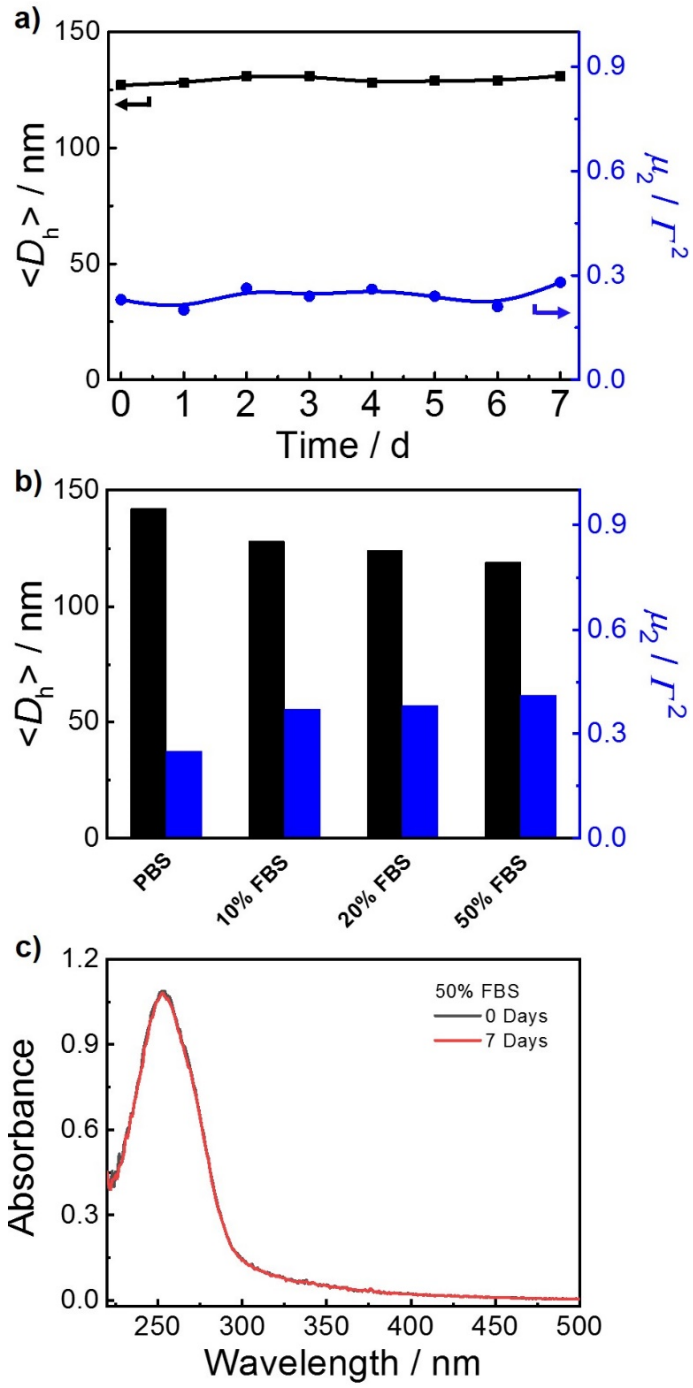

Figure S15. (a) Intensity-average hydrodynamic diameters, $<D_h>$, and polydispersity indexes, μ_2/Γ^2, recorded for **PQ2** vesicle upon storage over one week. (b) Intensity-average hydrodynamic diameters, $<D_h>$, and polydispersity indexes, μ_2/Γ^2, recorded for **PQ2** vesicles under various milieu conditions at 37 ºC. (c) UV-Vis absorption spectra recorded for **PQ2** vesicle dispersion (0.05 g/L) upon incubation with 50% FBS for one week at 37 ºC.

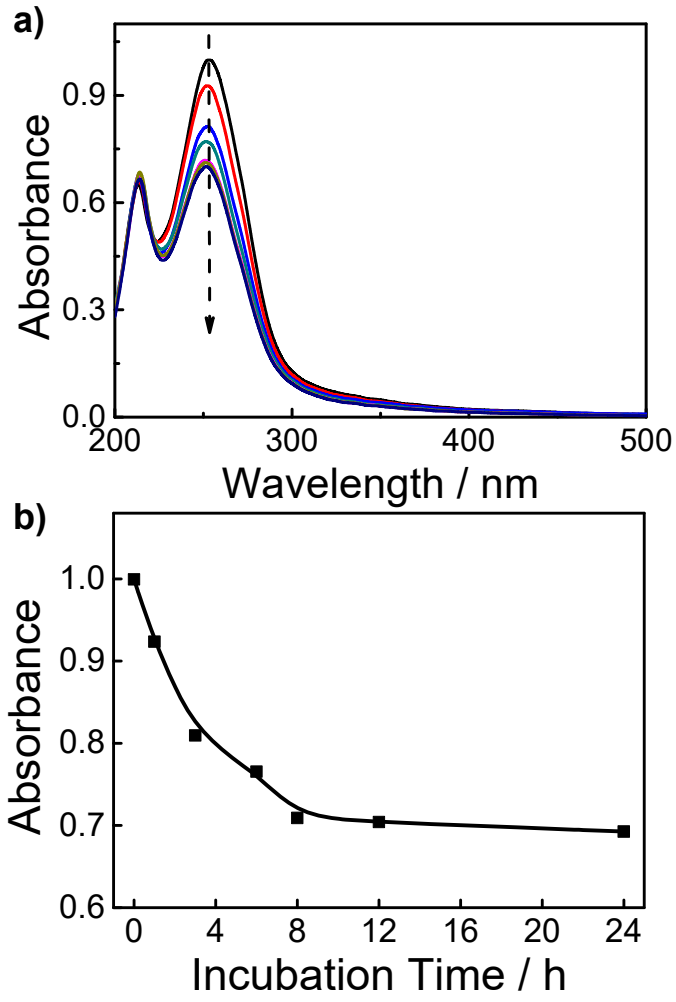

Figure S16. (a) UV-Vis absorption spectra recorded for **PQ2** vesicle dispersion (0.05 g/L) upon treating with NQO1 (80 μg/mL, 1 mM NADH, 0.007% BSA; pH 7.4 PBS, 100 mM KCl). (b) Time-dependent evolution of normalized absorbance intensities at 255 nm recorded for **PQ2** vesicle dispersion (0.05 g/L) upon treating with NQO1.

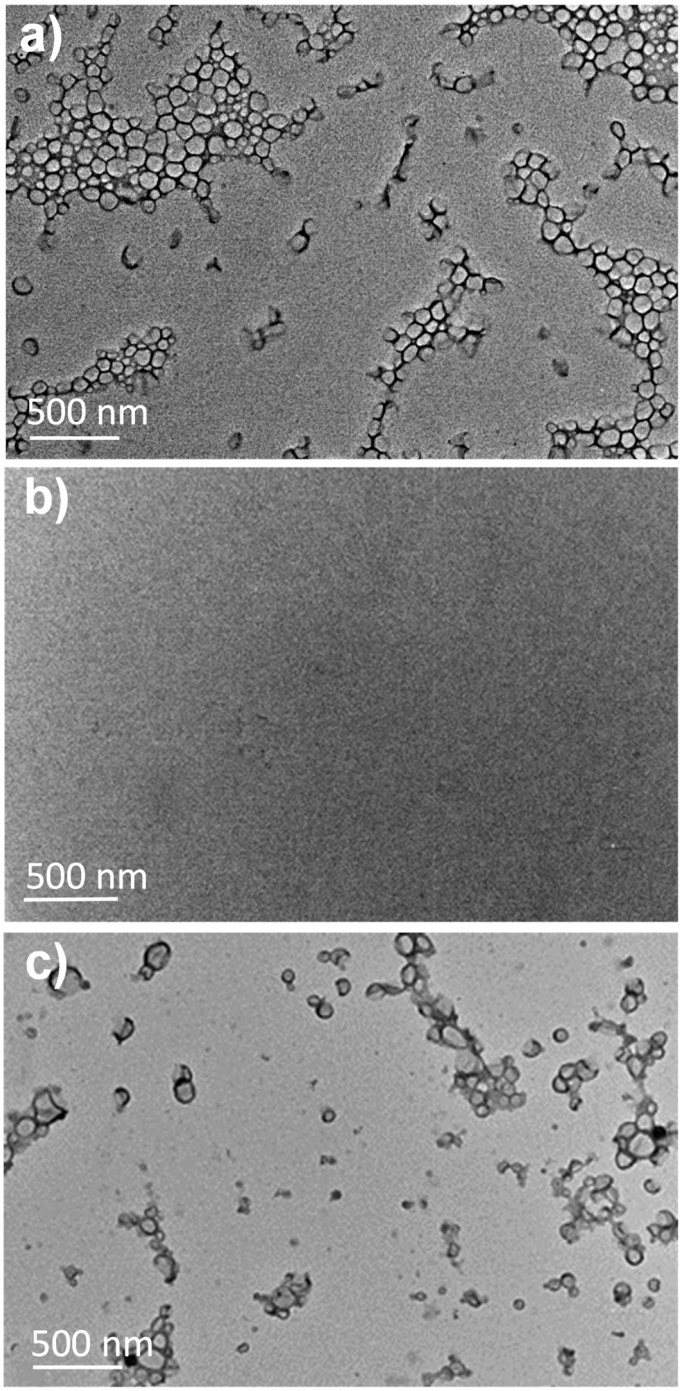

Figure S17. TEM images recorded for **PQ2** vesicles upon different treatments: (a) **PQ2** vesicles upon incubation with $NaBH_4$, (b) **PQ2** vesicular dispersion upon dilution with 19-fold DMF, (c) **PQ2** vesicular dispersion upon treating with $NaBH_4$, followed by 19-fold dilution with DMF.

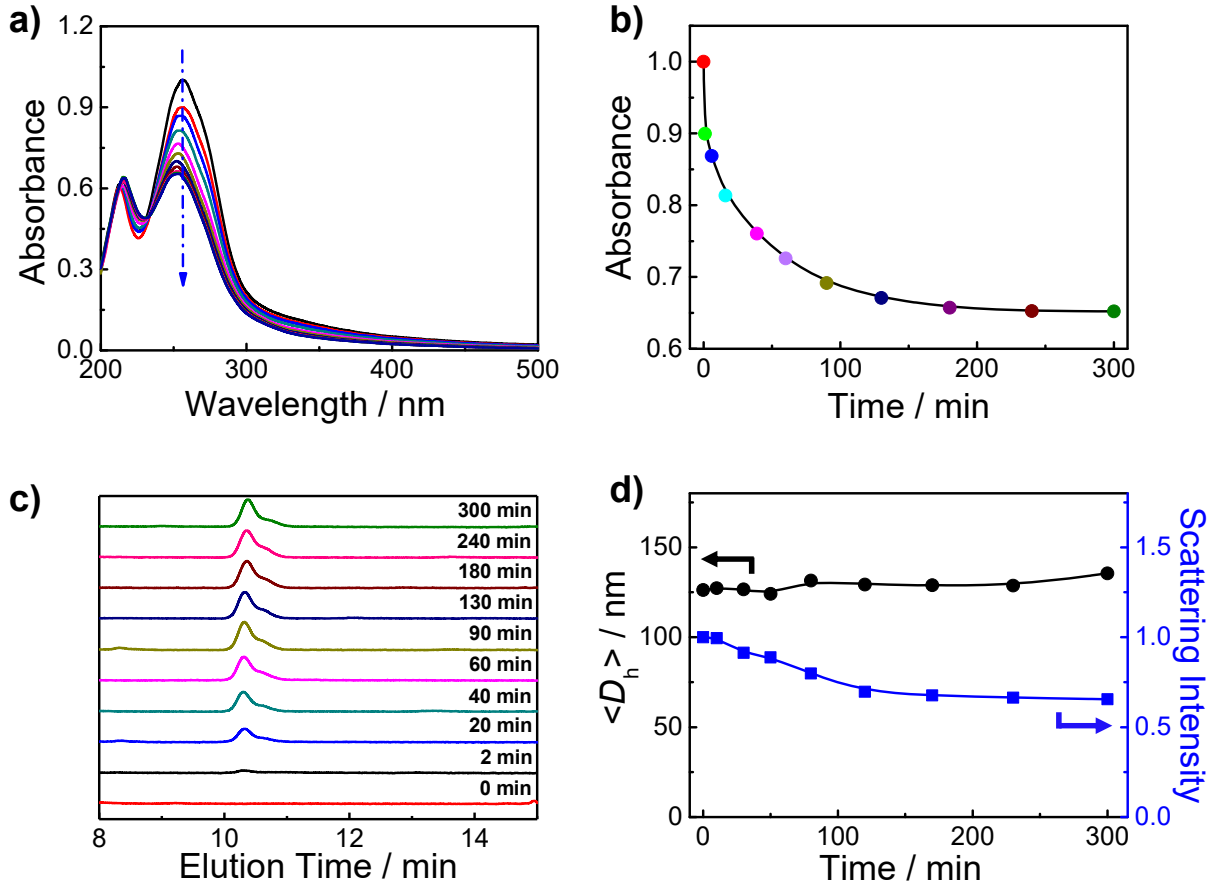

Figure S18. (a) UV-Vis absorption spectra recorded for **PQ2** vesicles in the presence of $NaBH_4$ (10 equiv. relative to TMQ moieties) in PB buffer (pH 7.4, 20 mM). (b) Time-dependent evolution of absorbance at 255 nm recorded for **PQ2** vesicle dispersion. (c) RP-HPLC traces recorded for released TMQL (elution time ~ 10.3 min) upon treating **PQ2** vesicles with $NaBH_4$ (10 equiv. relative to TMQ moieties) at 25 °C; mobile phase: MeOH/H_2O = 6/4; detection wavelength: 201 nm. (d) Time-dependent evolution of $<D_h>$ and normalized scattering light intensities recorded for **PQ2** vesicle dispersion (0.1 g/L) upon treating with $NaBH_4$ (10 equiv. relative to TMQ moieties; 25 °C).

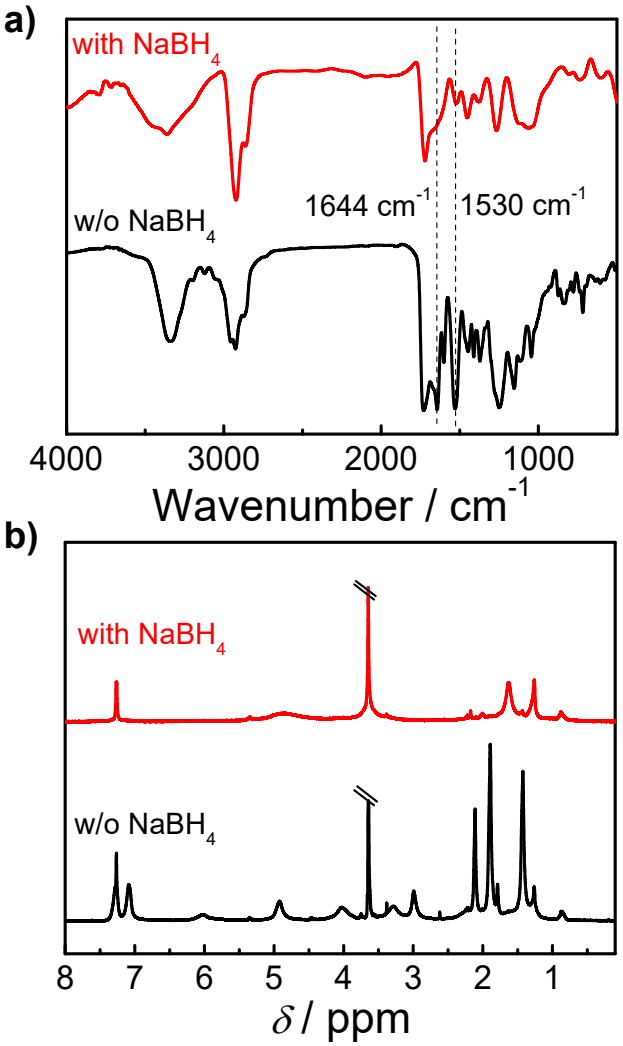

Figure S19. (a) FT-IR spectra and (b) ^{1}H NMR spectra recorded for **PQ2** vesicles before (black line) and after (red line) chemical reduction with $NaBH_4$ (10 equiv. relative to TMQ moieties, 25 ºC).

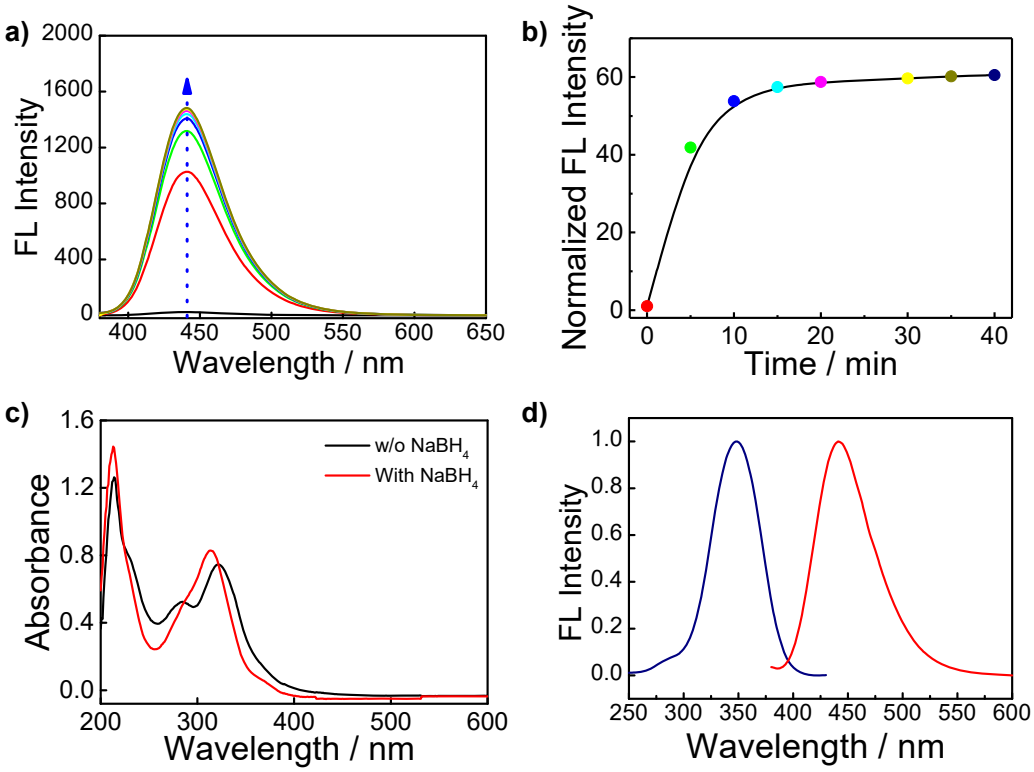

Figure S20. (a) Evolution of fluorescence emission spectra of **C5** precursor (10 μM) in PB buffer (pH 7.4, 20 mM) upon reduction with $NaBH_4$ (100 μM) (λ_{ex} = 370 nm, 25 °C). (b) Time-dependent changes of normalized fluorescence intensities at 440 nm upon treating **C5** precursor with $NaBH_4$. (c) UV-Vis absorption spectra recorded for **C5** precursor in PB buffer (pH 7.4, 20 λ_{em} = 440 nm) and emission spectrum (red line: λ_{ex} = 370 nm) recorded for 7-amino-4-methylcoumarin (AMC) in PB buffer (pH 7.4, 20 mM).

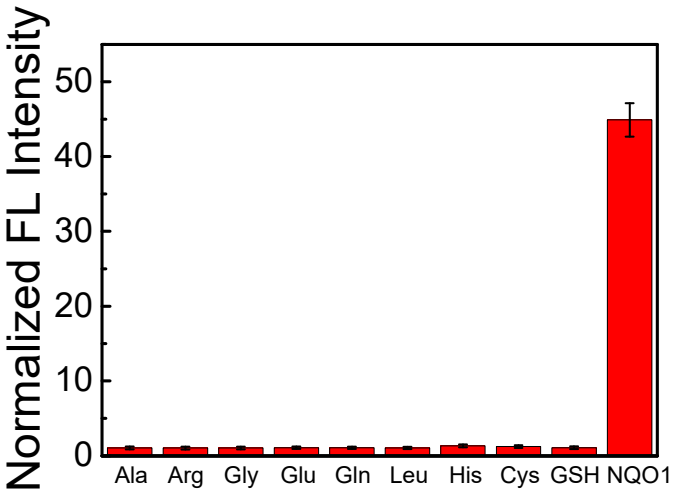

Figure S21. Fluorescence response assays recorded for CMA-conjugated **PQ5** vesicular dispersions upon treating with biological molecules and reductants (100 μM) for 24 h.

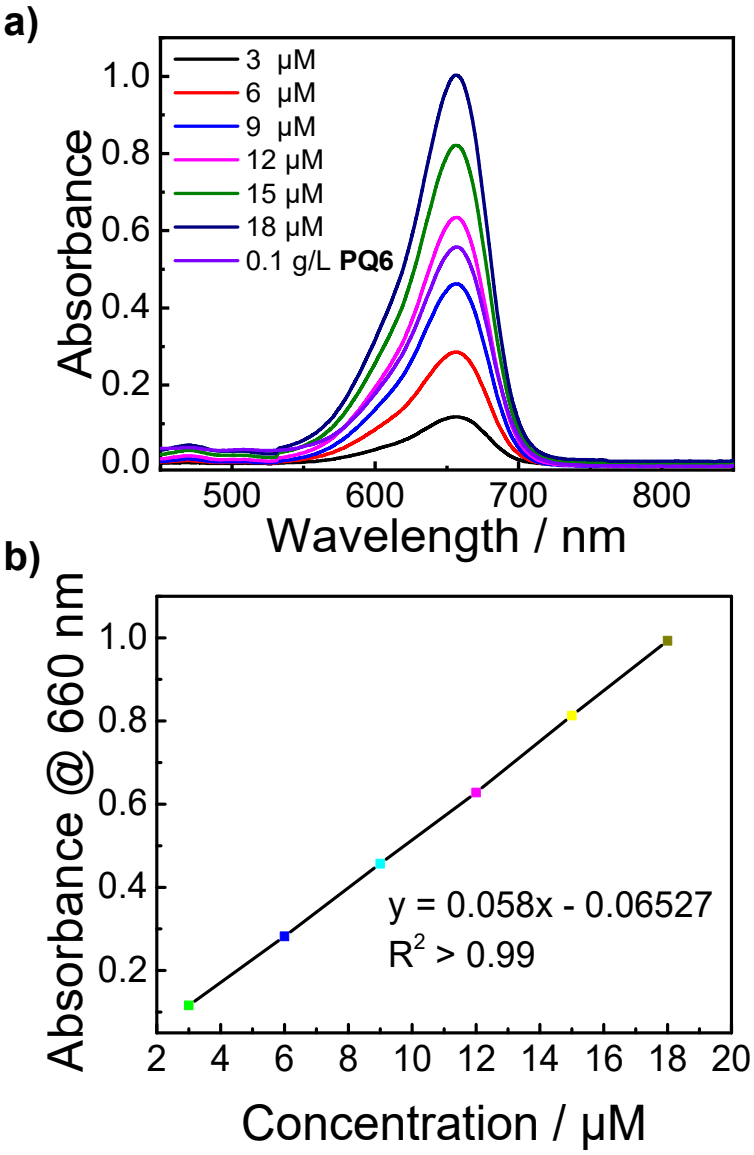

Figure S22. (a) UV-Vis absorption spectra recorded for **D3** at various concentrations (3-18 μM) and **PQ6** (0.1 g/L) in methanol. (b) The linear correlation between absorbance at 660 nm *versus* the concentration of **D3**.

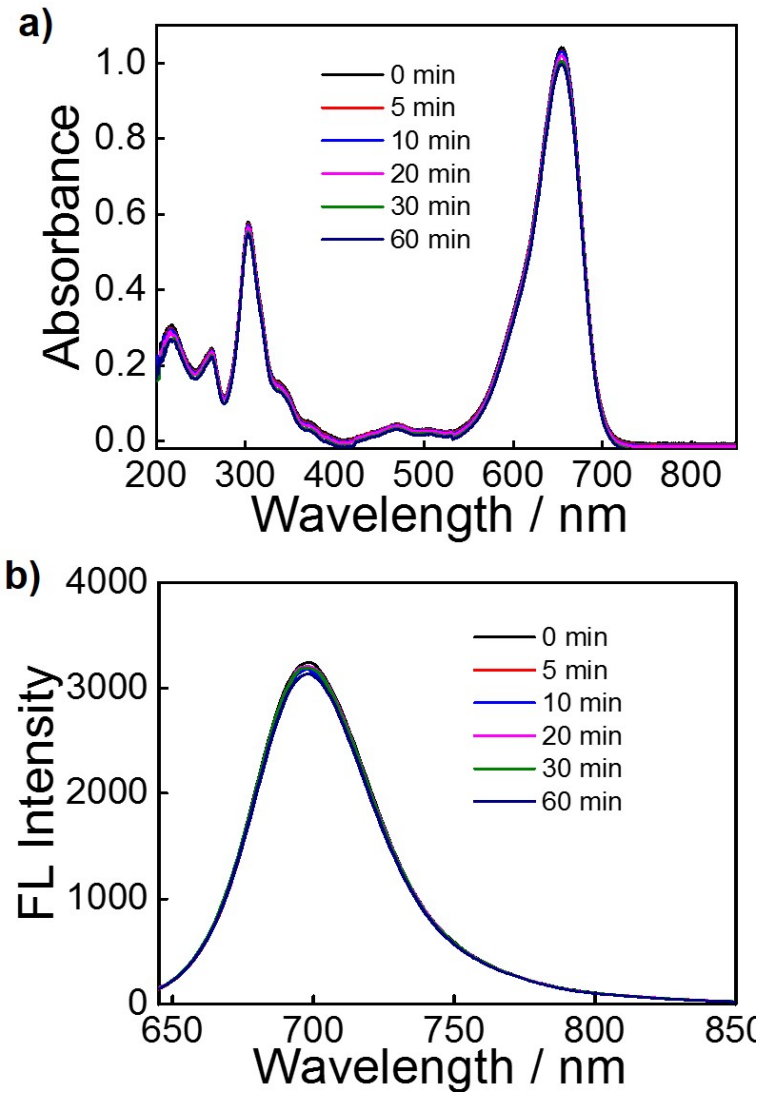

Figure S23. (a) UV-Vis absorption spectra and (b) fluorescence emission spectra recorded for **D3** in methanol under 660 nm LED light irradiation (20 mW/cm^2) for different durations (18 μM, λ_{ex} = 630 nm).

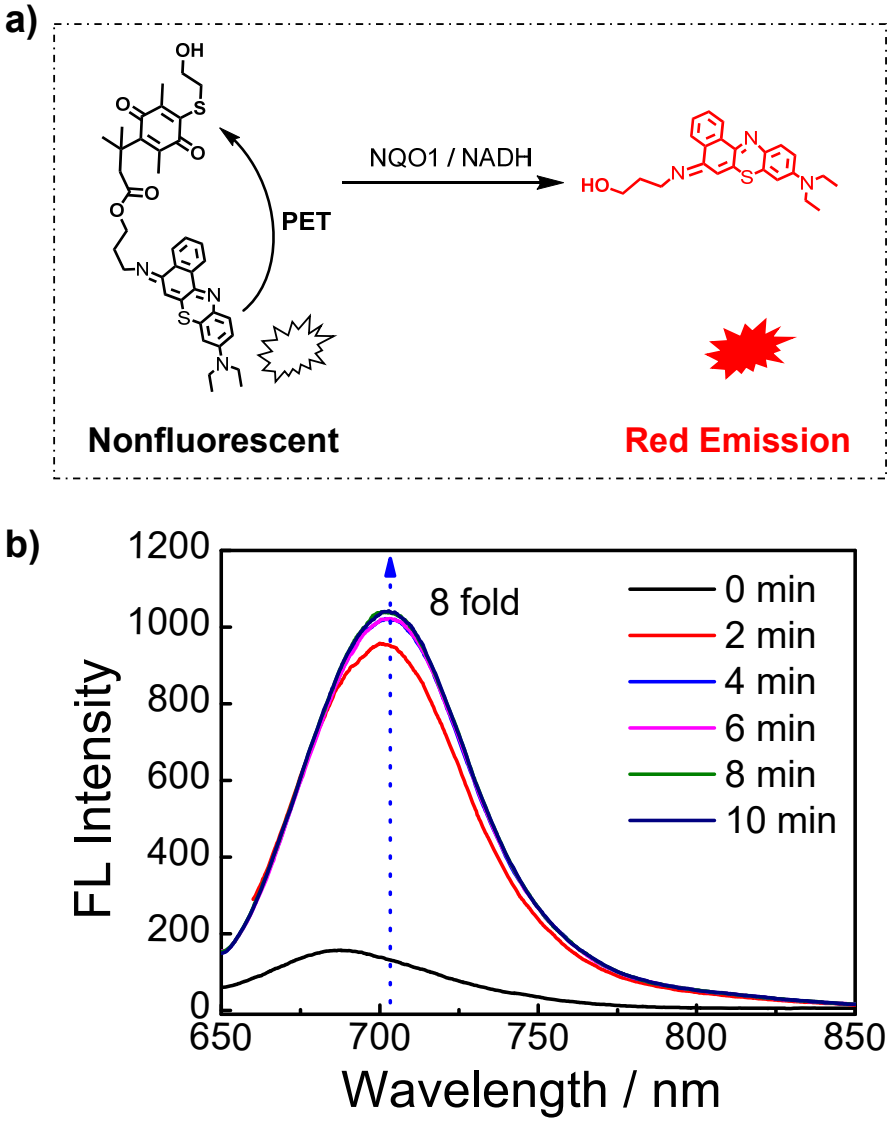

Figure S24. (a) Schematics of the PET quenching mechanism for **D3** precursor before and after reduction with NQO1 enzyme. (b) Time-dependent fluorescence recovery of **D3** (10 μM) upon incubation with NQO1 (5 μg/mL, 1 mM NADH, 0.007% BSA; pH 7.4 PBS, 100 mM KCl).

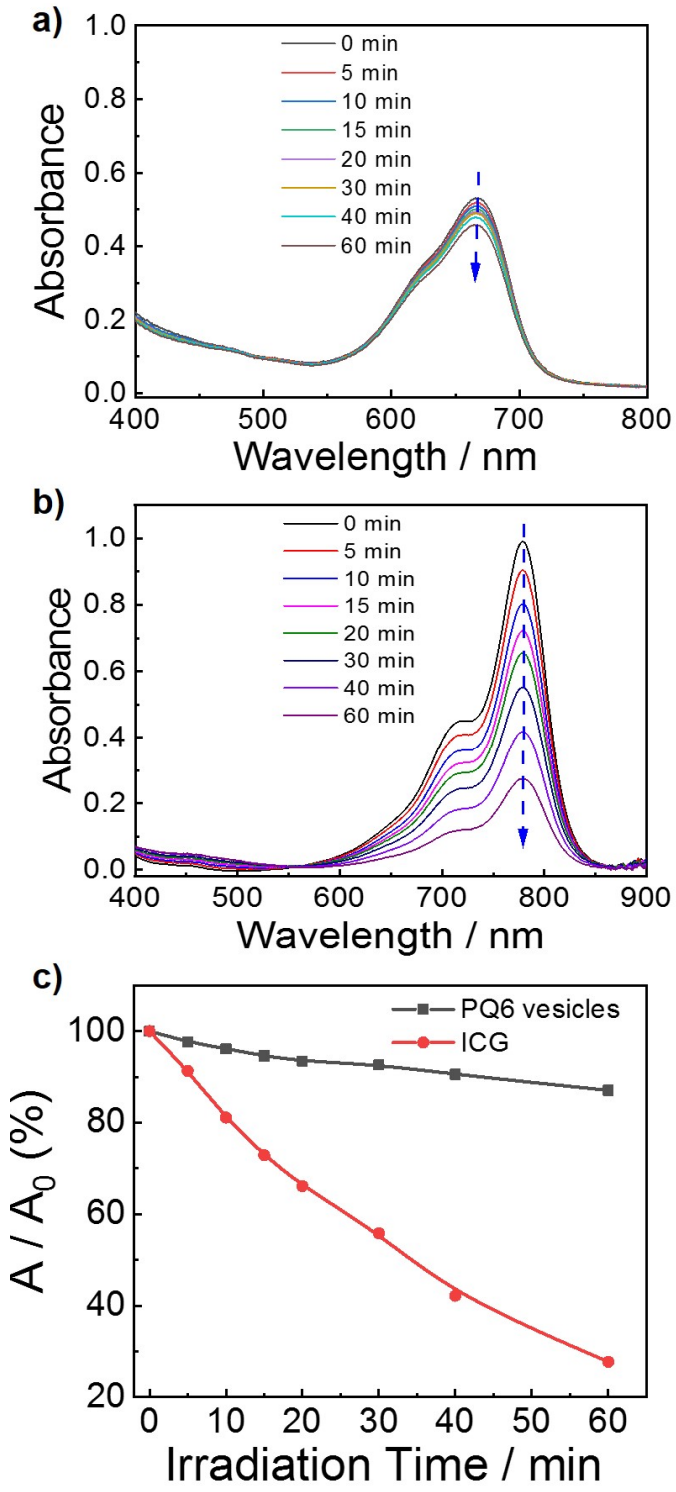

Figure S25. UV-Vis absorption spectra recorded for (a) **PQ6** vesicle dispersion (0.1 g/L) and (b) ICG (6 μM) in PB buffer (pH 7.4, 10 mM) under 660 nm light irradiation (200 mW/cm^2) for varying durations. (c) Time-dependent changes of normalized absorbance at 660 nm for **PQ6** vesicles and 780 nm for ICG in (a) and (b), respectively.

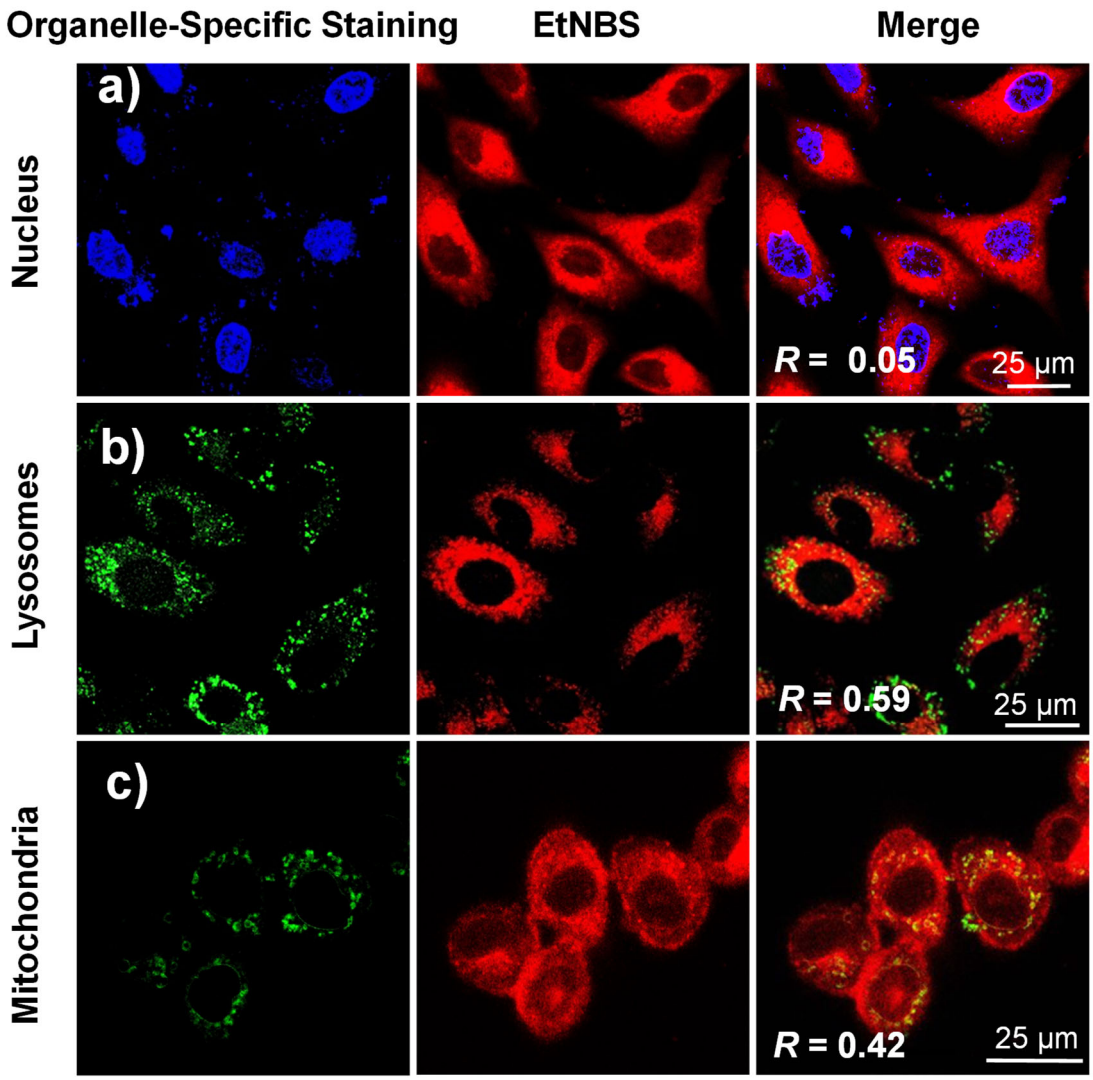

Figure S26. Subcellular colocalization assays of A549 cells upon additional 20 h incubation followed by 4 h co-incubation with **PQ6** vesicles (0.2 g/L). CLSM images were recorded for **PQ6** vesicles (EtNBS channel) and intracellular organelles, and corresponding colocalization analysis results were also included: (a) Cell nuclei co-stained with DAPI (λ_{ex} = 405 nm, λ_{em} = 440 ± 20 nm); (b) Lysosomes co-stained with LysoTracker Green (λ_{ex} = 488 nm, λ_{em} = 520 ±20 nm); (c) Mitochondria co-stained by MitoTracker Green (λ_{ex} = 488 nm, λ_{em} = 520 ± 20 nm). The colocalization ratios were denoted as *R* in merged CLSM images.

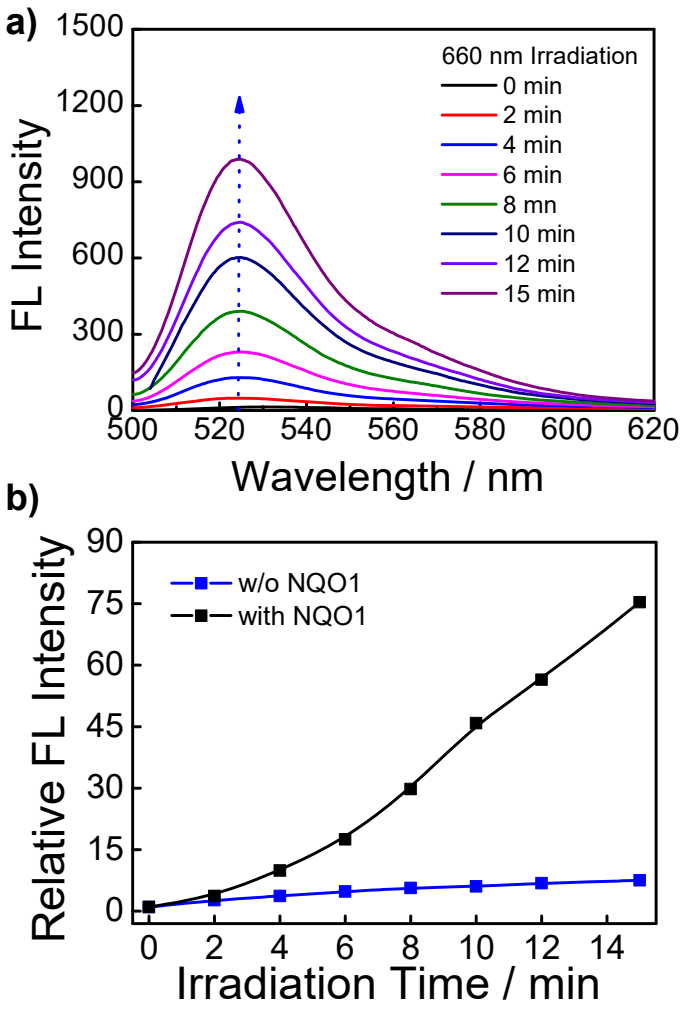

Figure S27. (a) Evolution of fluorescence emission spectra (λ_{ex} = 480 nm) recorded for DCFH-DA probe (12 μM) in NQO1-treated vesicular dispersion of **PQ6** (0.05 g/L, ~4.6 μM EtNBS) upon 660 nm LED light irradiation (20 mW/cm^2). (b) Time-dependent changes of normalized emission intensities (λ_{em} = 525 nm) recorded for DCFH-DA probe in non-treated and NQO1-treated **PQ6** vesicular dispersions (0.05 g/L, ~4.6 μM EtNBS) upon 660 nm light irradiation (20 mW/cm^2). The **PQ6** vesicular dispersion was co-incubated with NQO1 enzyme for 24 h before 660 nm light irradiation.

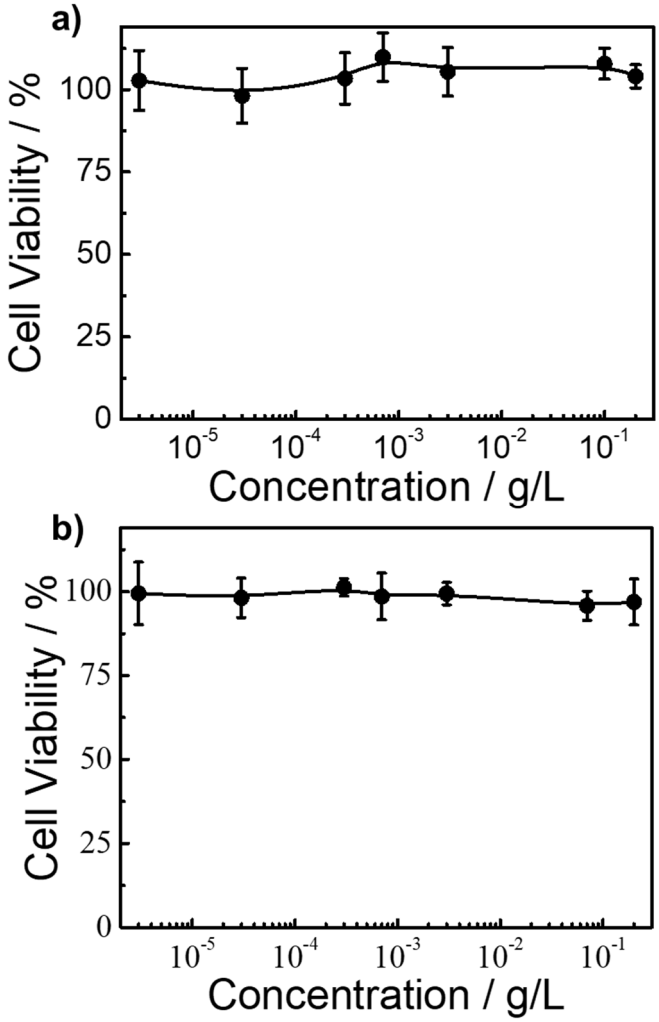

Figure S28. *In vitro* cytotoxicity of A549 cells upon co-incubation with **PQ2** vesicles for (a) 48 h and (b) 72 h, respectively.

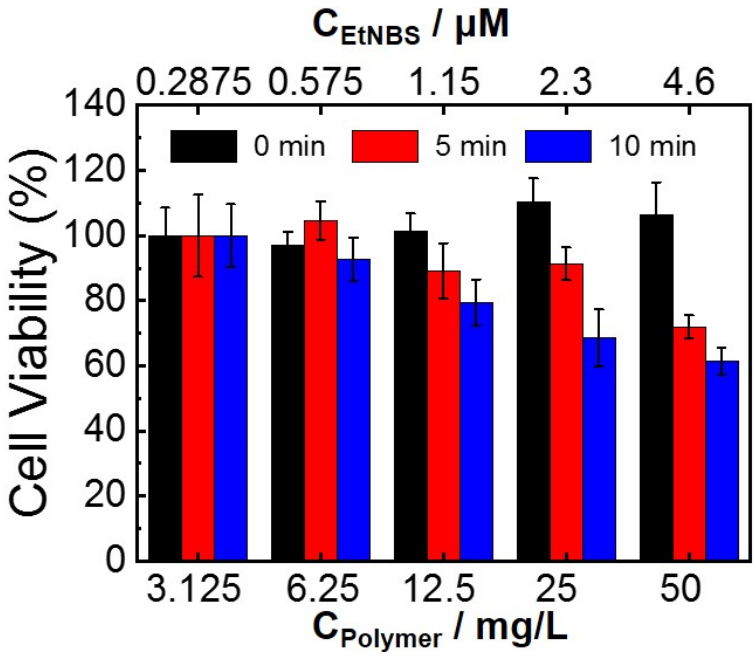

Figure S29. Viability of H596 cells upon incubation for an additional 20 h after 4 h co-incubation with **PQ6** vesicle dispersions at varying concentrations, and then irradiated with 660 nm light (20 mW/cm^2) for specified time intervals.

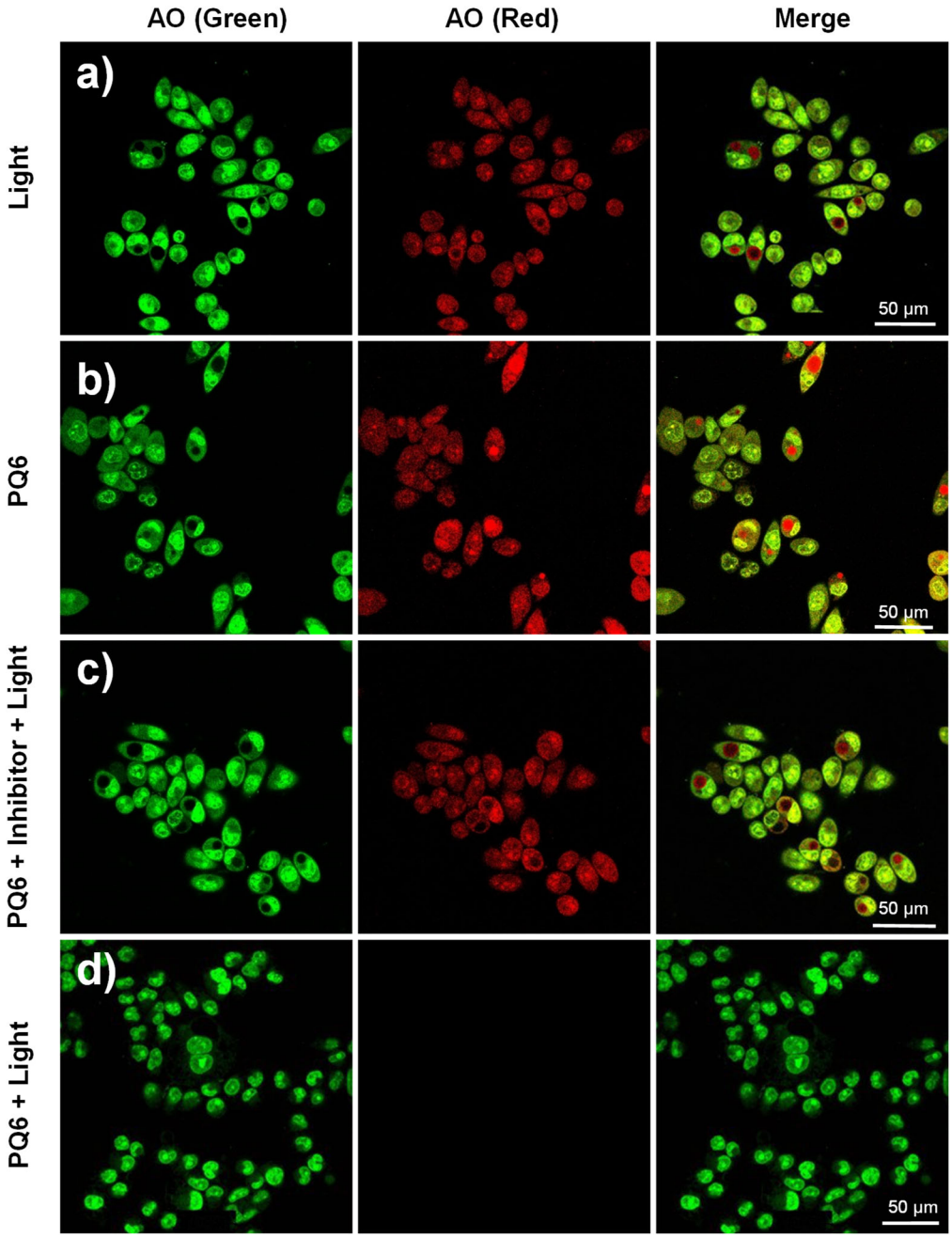

Figure S30. Representative green channel (λ_{ex} = 488 nm, λ_{em} = 520 ±20 nm) and red channel (λ_{ex} = 543 nm, λ_{em} = 630 ± 20 nm) CLSM images recorded for acridine orange (AO)-stained A549 cells, revealing lysosomal integrity after different treatments: (a) 660 nm light irradiation for 10 min; (b) co-incubation with **PQ6** vesicle dispersion (0.2 g/L); (c) Pretreated with dicoumarol (50 µM) for 1 h and then incubation for an additional 20 h after 4 h co-incubation with **PQ6** vesicular dispersion (0.2 g/L), followed by 660 nm light irradiation for 10 min. (d) Incubation for an additional 20 h after 4 h co-incubation with **PQ6** vesicular dispersion, followed by 660 nm light irradiation for 10 min (20 mW/cm^2).

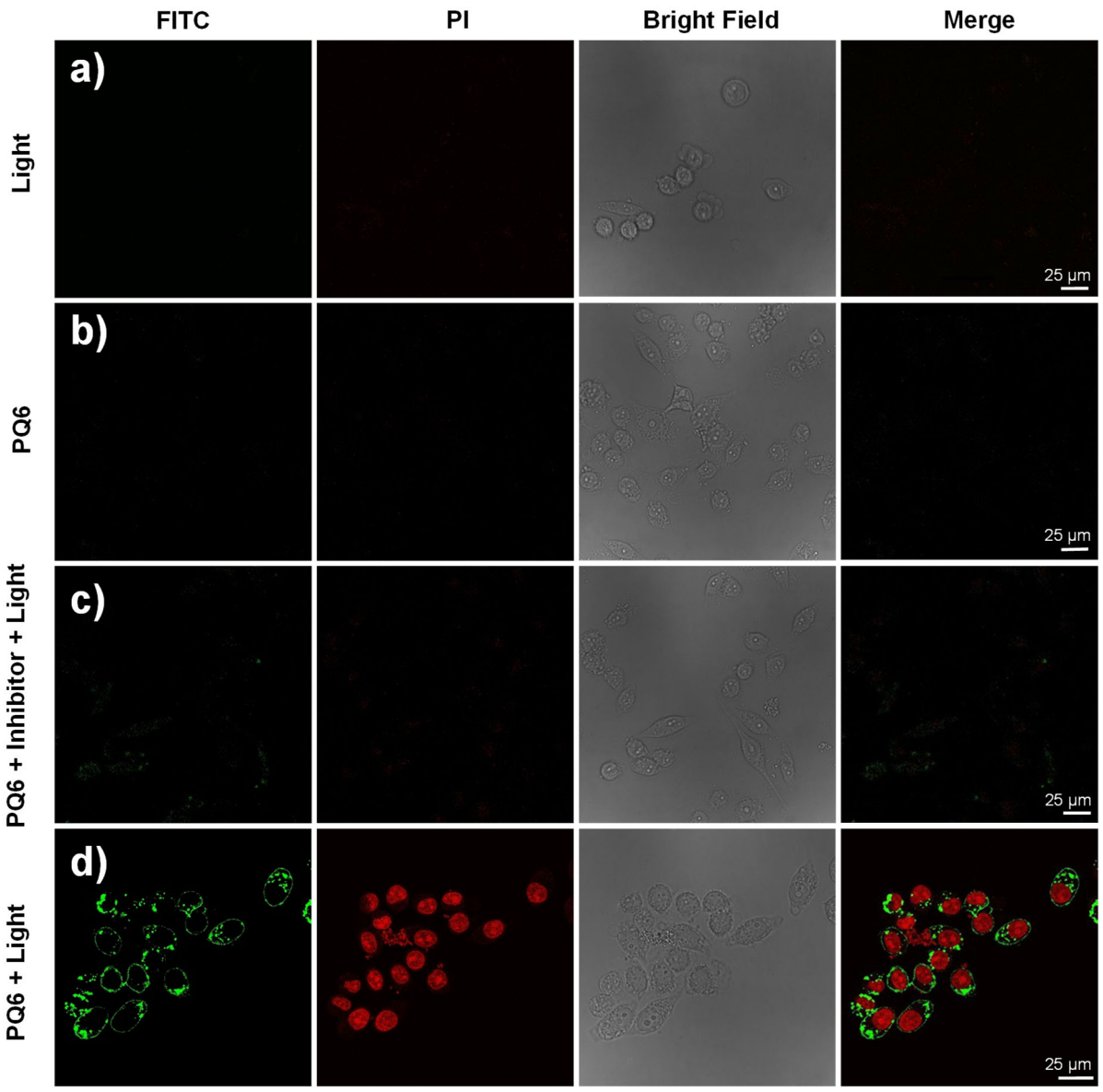

Figure S31. CLSM images recorded for A549 cells upon different treatments, and then stained with Annexin V-FITC (λ_{ex} = 488 nm, λ_{em} = 520 ±20 nm) and PI (λ_{ex} = 543 nm, λ_{em} = 580 ±20 nm): (a) 660 nm light irradiation for 10 min; (b) co-incubation with **PQ6** vesicle dispersion (0.2 g/L); (c**)** Pretreated with dicoumarol (50 μM) for 1 h and then incubation for an additional 20 h after 4 h co-incubation with **PQ6** vesicular dispersion (0.2 g/L), followed by 660 nm light irradiation for 10 min; (d) Incubation for an additional 20 h after 4 h co-incubation with **PQ6** vesicular dispersion, followed by 660 nm light irradiation for 10 min (20 mW/cm^2).

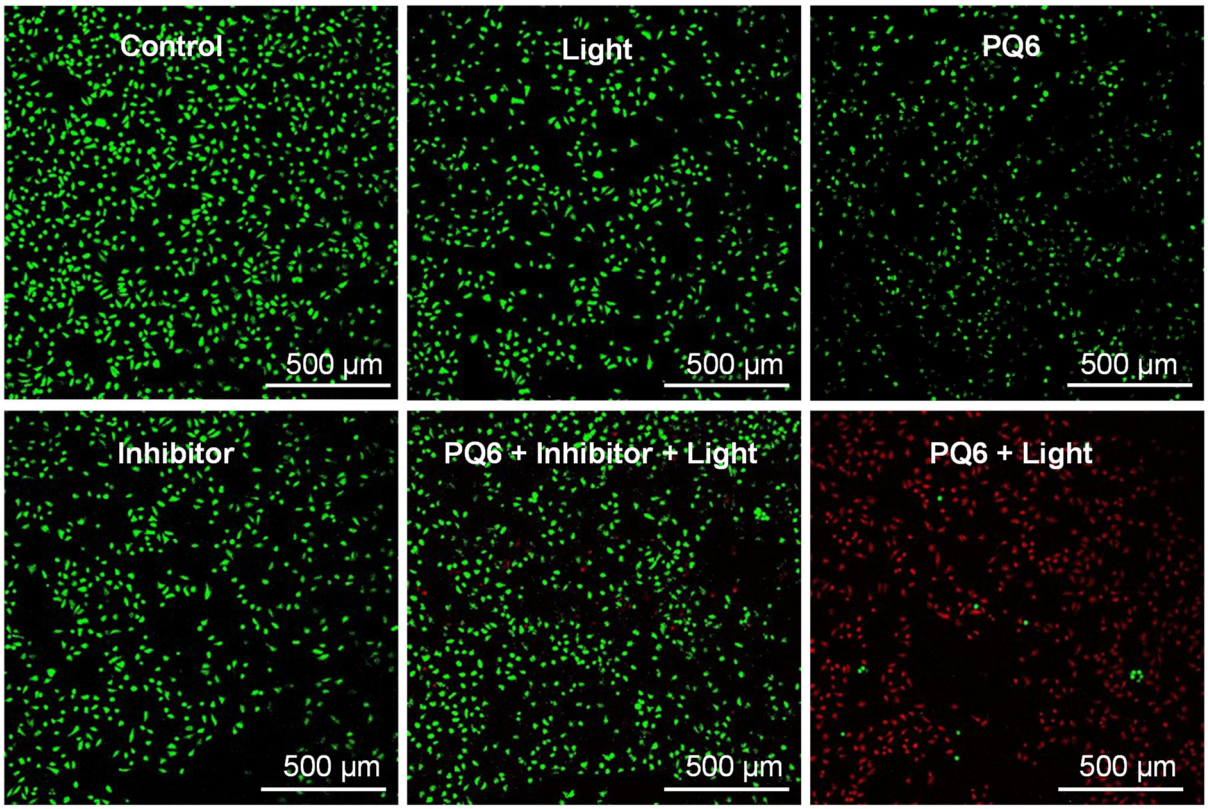

Figure S32. Live/dead assays recorded for A549 cells upon different treating protocols in the absence and presence of **PQ6** vesicles (0.05 g/L). Light irradiation was performed in three treating groups (660 nm, 20 mW/cm^2, 10 min). In two cases, cells were pretreated with dicoumarol inhibitor (50 μM) for 1 h at first to inhibit the activity of intracellular NQO1 enzyme, followed by co-incubation with **PQ6** vesicles.

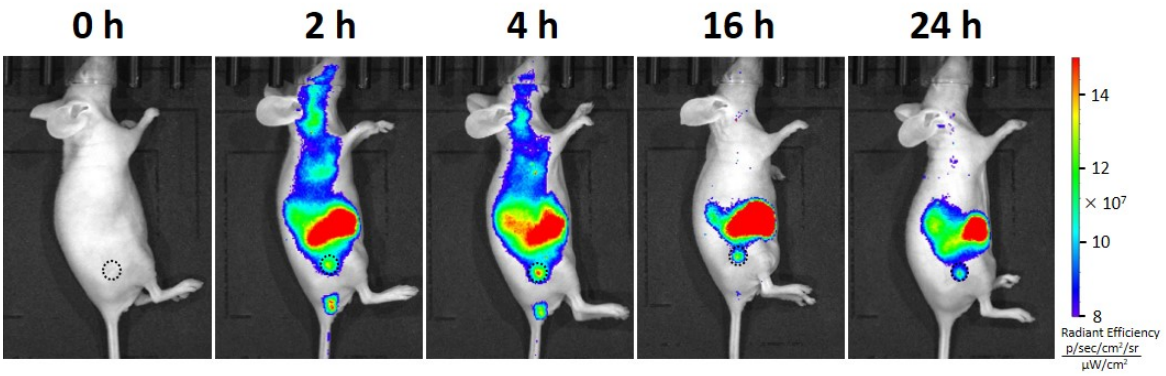

Figure S33. (a) *In vivo* NIR fluorescence tumor imaging of A549 tumor-bearing nude mice at 2, 4, 16, and 24 h after intravenous injection of **PQ6** vesicle dispersion (100 µL, 2.0 g/L).

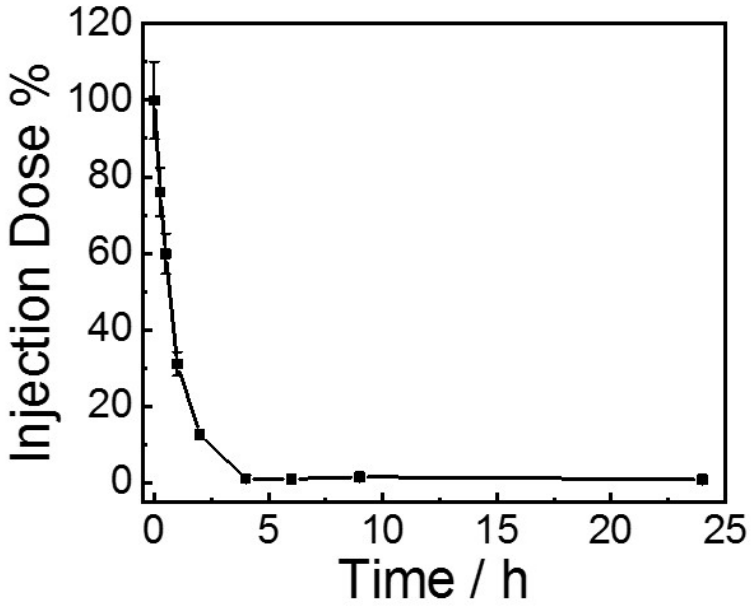

Figure S34. Blood clearance kinetics profile of **PQ6** vesicle dispersion after intravenous injection into Balb/c female mice (a dose of 10 mg/kg). The data are presented as the average ± standard error (n = 3).

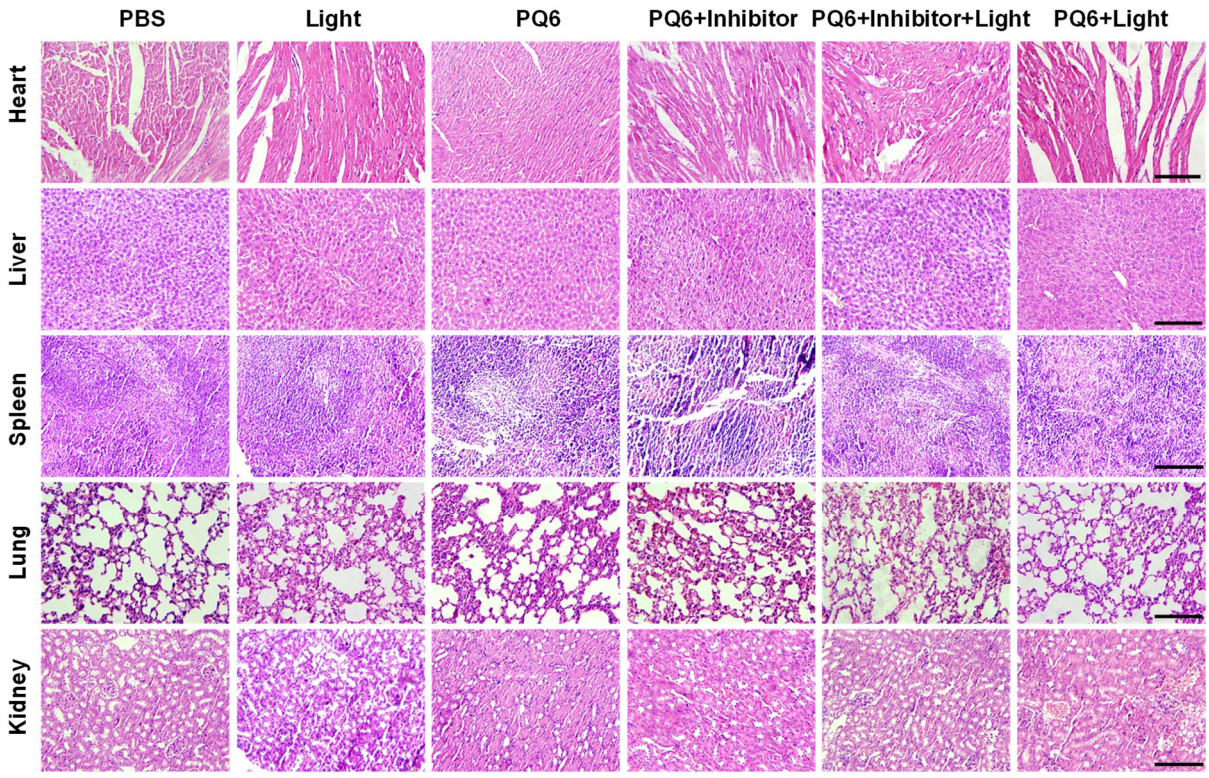

Figure S35. Typical H&E staining images (scale bar: 200 μm) recorded for major organs of mice including heart, liver, spleen, lung, and kidney after different treating protocols.

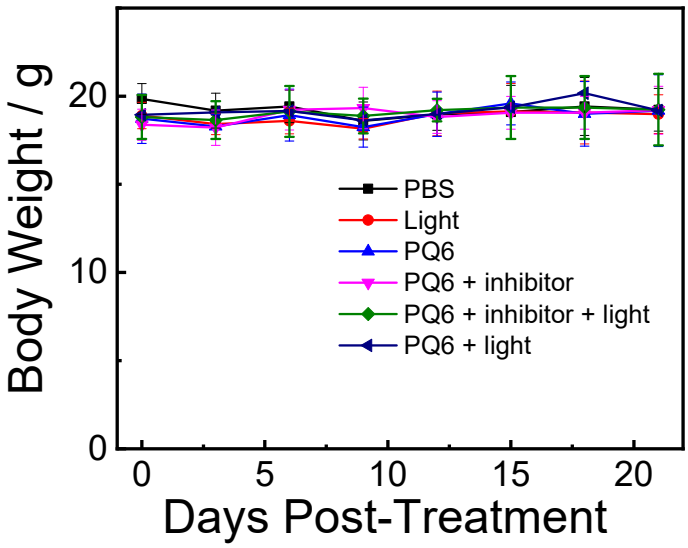

Figure S36. Evolution of the body weights of A549 tumor-bearing mice upon different treating protocols. No obvious fluctuations of body weights were observed in all treating groups.

References

1. Convertine, A. J.; Lokitz, B. S.; Vasileva, Y. L.; Myrick, L. J.; Scales, C. W.; Lowe, A. B.; McCormick, C. L. Direct Synthesis of Thermally Responsive DMA/NIPAM Diblock and DMA/NIPAM/DMA Triblock Copolymers *via* Aqueous, Room Temperature RAFT Polymerization. *Macromolecules* **2006**, *39*, 1724-1730.

2. Louis A. Carpino, S. A. T., and Richard A. Berglund. Reductive Lactonization of Strategically Methylated Quinone Propionic Acid Esters and Amides. *J. Org. Chem.* **1988**, *54*, 3303-3310.

3. Verma, S.; Sallum, U. W.; Athar, H.; Rosenblum, L.; Foley, J. W.; Hasan, T. Antimicrobial Photodynamic Efficacy of Side-Chain Functionalized Benzo[a]Phenothiazinium Dyes. *Photochem. Photobiol.* **2009**, *85*, 111-118.

4. Yu, S. S.; Lau, C. M.; Barham, W. J.; Onishko, H. M.; Nelson, C. E.; Li, H.; Smith, C. A.; Yull, F. E.; Duvall, C. L.; Giorgio, T. D. Macrophage-Specific RNA Interference Targeting *via* "Click", Mannosylated Polymeric Micelles. *Mol. Pharm.* **2013**, *10*, 975-987.

5. Walton, D. P.; Dougherty, D. A. A General Strategy for Visible-Light Decaging Based on the Quinone Trimethyl Lock. *J. Am. Chem. Soc.* **2017**, *139*, 4655-4658.

6. Prasuhn, D. E., Jr.; Yeh, R. M.; Obenaus, A.; Manchester, M.; Finn, M. G. Viral Mri Contrast Agents: Coordination of Gd by Native Virions and Attachment of Gd Complexes by Azide-Alkyne Cycloaddition. *Chem. Commun.* **2007**, 1269-1271.

7. Haupler, B.; Ignaszak, A.; Janoschka, T.; Jahnert, T.; Hager, M. D.; Schubert, U. S. Poly(Methacrylates) with Pendant Benzoquinone Units - Monomer Synthesis, Polymerization, and Electrochemical Behavior: Potential New Polymer Systems for Organic Batteries. *Macromol. Chem. Phys.* **2014**, *215*, 1250-1256.